Simultaneous Brain, Brainstem and Spinal Cord pharmacological-fMRI reveals involvement of an endogenous opioid network in attentional analgesia

Valeria Oliva[1,2,6], Ron Hartley-Davies[2,3], Rosalyn Moran[4], Anthony E. Pickering[1], Jonathan C.W. Brooks[2,5]

1) Anaesthesia, Pain & Critical Care Sciences, School of Physiology, Pharmacology & Neuroscience, Biomedical Sciences Building, University of Bristol, Bristol, BS8 1TD, UK.
2) Clinical Research and Imaging Centre, School of Psychological Science, University of Bristol, Bristol, BS8 1TU, UK
3) Medical Physics, University Hospitals Bristol & Weston NHS Trust, Bristol, BS2 8HW, UK.
4) Department of Neuroimaging, Institute of Psychiatry, Psychology & Neuroscience, King's College London, London, SE5 8AF, UK.
5) Wellcome Wolfson Brain Imaging Centre, School of Psychology, Lawrence Stenhouse Building, University of East Anglia, Norwich, NR4 7TJ, UK.
6) Department of Anesthesiology, University of California San Diego, 9500 Gilman Dr, La Jolla, CA 92093, USA.

Corresponding Author: AE Pickering

Summary

Pain perception is decreased by shifting attentional focus away from a threatening event. This attentional analgesia engages parallel descending control pathways from anterior cingulate (ACC) to locus coeruleus, and ACC to periaqueductal grey (PAG) – rostral ventromedial medulla (RVM), indicating possible roles for noradrenergic or opioidergic neuromodulators. To determine which pathway modulates nociceptive activity in humans we used simultaneous whole brain-spinal cord pharmacological-fMRI (N=39) across three sessions. Noxious thermal forearm stimulation generated somatotopic-activation of dorsal horn (DH) whose activity correlated with pain report and mirrored attentional pain modulation. Activity in an adjacent cluster reported the interaction between task and noxious stimulus. Effective connectivity analysis revealed that ACC interacts with PAG and RVM to modulate spinal cord activity. Blocking endogenous opioids with Naltrexone impairs attentional analgesia and disrupts RVM-spinal and ACC-PAG connectivity. Noradrenergic augmentation with Reboxetine did not alter attentional analgesia. Cognitive pain modulation involves opioidergic ACC-PAG-RVM descending control which suppresses spinal nociceptive activity.

Introduction

Pain is a fundamental and evolutionarily conserved cognitive construct that is behaviourally prioritised by organisms to protect themselves from harm and facilitate survival. As such pain perception is sensitive to the context within which potential harm occurs. There are well recognised top-down influences on pain that can either suppress (e.g. placebo (Wager and Atlas, 2015) or task engagement (Bussing et al., 2010)) or amplify (e.g. catastrophising (Gracely et al., 2004), hypervigilance (Crombez et al., 2004) or nocebo (Benedetti and Piedimonte, 2019)) its expression. These processes influence both acute and chronic pain and provide a dynamic, moment by moment regulation of pain as an organism moves through their environment.

A simple shift in attention away from a noxious stimulus can cause a decrease in pain perception – a phenomenon known as attentional analgesia. This effect can be considered to be a mechanism to enable focus, allowing prioritisation of task performance over pain interruption (Eccleston and Crombez, 1999; Erpelding and Davis, 2013). This phenomenon is reliably demonstrable in a laboratory setting (Miron et al., 1989) and a network of cortical and brainstem structures have been implicated in attentional analgesia (Bantick et al., 2002; Brooks et al., 2017; Bushnell et al., 2013; Lorenz et al., 2003; Petrovic et al., 2002; Peyron et al., 2000; Sprenger et al., 2012; Tracey et al., 2002; Valet et al., 2004).

We have shown that two parallel pathways are implicated in driving brainstem activity related to attentional analgesia (Brooks et al., 2017; Oliva et al., 2021b). Projections from rostral anterior cingulate cortex (ACC) were found to drive the periaqueductal grey (PAG) and rostral ventromedial medulla (RVM), which animal studies have shown to work in concert using opioidergic mechanisms to regulate spinal nociception (Fields, 2004; Fields and Basbaum, 1978; Heinricher et al., 1994; Ossipov et al., 2010). Similarly, a bidirectional connection between ACC and locus coeruleus (LC) was also directly involved in attentional analgesia. As the primary source of cortical noradrenaline, the LC is thought to signal salience of incoming sensory information (Aston-Jones and Cohen, 2005; Sara and Bouret, 2012), but can also independently modulate spinal nociception (De Felice et al., 2011; Hirschberg et al., 2017; Hughes et al., 2015; Llorca-Torralba et al., 2016). Although these

animal studies provide a framework for our understanding of descending control mechanisms that are likely to be mediating attentional analgesia, the network interactions between brain, brainstem and spinal cord and the neurotransmitter systems involved in producing attentional analgesia have yet to be elucidated in humans. In part, this gap in our knowledge is because of the distributed extent of the network spanning the entire neuraxis from forebrain to spinal cord, which has only relatively recently become accessible using simultaneous imaging approaches in humans (Cohen-Adad et al., 2010; Finsterbusch et al., 2013; Islam et al., 2019).

To address this issue, we conducted a double-blind, placebo-controlled, three arm, cross-over pharmacological-fMRI experiment to investigate attentional analgesia using whole neuraxis imaging and a well validated experimental paradigm. To engage attention, we utilised a rapid serial visual presentation (RSVP) task (Brooks et al., 2017; Oliva et al., 2021b; Potter and Levy, 1969) with individually calibrated task difficulties (easy or hard), which was delivered concurrently with thermal stimulation (low or high), adjusted per subject, to evoke different levels of pain. We took advantage of recent improvements in signal detection (Duval et al., 2015) and pulse sequence design to simultaneously capture activity across the brain, brainstem, and spinal cord (i.e. whole central nervous system, CNS) in a single contiguous functional acquisition with slice-specific z-shimming (Finsterbusch et al., 2012). To resolve the relative contributions from the opioidergic and noradrenergic systems, subjects received either the opioid antagonist naltrexone (which we predicted would block attentional analgesia), the noradrenaline re-uptake inhibitor reboxetine (which we expected to augment attentional analgesia), or placebo control. By measuring the influence of these drugs on pain perception, BOLD activity and effective connectivity between a priori specified regions known to be involved in attentional analgesia (ACC, PAG, LC, RVM, spinal cord (Brooks et al., 2017; Oliva et al., 2021b; Sprenger et al., 2012)), we sought to identify the network interactions and neurotransmitter mechanisms mediating this cognitive modulation of pain.

Results

A total of 39 subjects (mean age 23.7, range [18 - 45] years, 18 females) completed the three fMRI imaging sessions with a 2x2 factorial experimental design (RSVP task difficulty: easy or hard, thermal stimulus intensity: low or high, Figure 1). A different drug was administered orally before each scan session (naltrexone (50mg), reboxetine (4mg) or placebo), which included whole CNS imaging with slice-specific z-shimming (see Figure 1 Supplementary Figure 1).

The behavioural signature of attentional analgesia is a task*temperature interaction, driven by a reduction in pain ratings during the high temperature-hard task condition (Brooks et al., 2017; Oliva et al., 2021a; Oliva et al., 2021b). A first level analysis of the pooled pain behavioural data across all experimental sessions showed: a main effect of temperature ($F(1,38) = 221$, $P=0.0001$, Figure 2 Supplementary Figure 1) with higher scores under the high temperature conditions; a main effect of task ($F(1,38) = 4.9$, $P=0.03$); and importantly demonstrated the expected task*temperature interaction consistent with attentional pain modulation ($F(1, 38) = 10.5$, $P = 0.0025$, Figure 2 Supplementary Figure 1).

To assess the impact of the drugs on attentional analgesia, each experimental session was analysed independently (Figure 2A). Attentional analgesia was seen in the placebo condition (task*temperature interaction ($F(1, 38) = 11.20$, $P = 0.0019$), driven primarily by lower pain scores in the hard|high vs easy|high condition (37.5±19.4 vs 40.4±19.8, mean±SD, $P = 0.001$, effect size of -0.55 (Cohen's D_z)). Similarly, subjects given Reboxetine showed a task*temperature interaction ($F(1, 38) = 9.023$, $P = 0.0047$), again driven by decreased pain scores in the hard|high vs easy|high condition (31.9 ± 15.8 vs 35.6 ± 15.5, $P = 0.0034$, D_z=-0.42). In contrast, Naltrexone blocked the analgesic effect of attention with no task*temperature interaction ($F(1, 38) = 0.4355$, $P = 0.5133$, hard|high (37.4±17.1) vs easy|high (38.3±17.1), D_z=-0.11). Further analysis of the attentional modulation of pain showed that subjects in both the placebo and reboxetine conditions showed a significant decrease in pain score during the hard task that was not evident in the presence of naltrexone (Figure 2 Supplementary Figure 2, one sample t-test). We used equivalence analysis (TOST method described by Lakens (2017)) to demonstrate that the plausible magnitude of the attentional analgesic effect under naltrexone was smaller than a 6% (<2.3

point) reduction in pain score (P=0.049) confirming it as being smaller than that seen in the presence of placebo or reboxetine. This effect was specific to attentional analgesia as naltrexone had no effect on the calibrated temperature for the high thermal stimulus or the speed of character presentation for the RSVP task (Figure 2 Supplementary Figure 3). Behaviourally these findings indicate that the attentional analgesic effect is robust, reproducible between and across subjects and that it involves an opioidergic mechanism.

We also noted a drug*temperature interaction on pain ratings in the first level analysis ($F(2, 76) = 3.2$, $P = 0.04$, Figure 2 Supplementary Figure 1). Comparing reboxetine versus placebo showed the presence of a drug*temperature interaction ($F(1, 38) = 5.060$, $P = 0.03$, Figure 2), with lower pain scores in the presence of reboxetine indicating that it was underpinned by an analgesic effect of the noradrenergic reuptake inhibitor (in contrast naltrexone vs placebo showed no drug*temperature interaction).

Whole CNS fMRI: main effects and interactions

To determine the neural substrates for attentional analgesia and to identify the possible involvement of the noradrenergic and opioidergic systems, we initially defined a search volume in which to focus subsequent detailed fMRI analyses. This was achieved by pooling individually averaged data across the three experimental imaging sessions to estimate main effects and interactions across all levels of the neuraxis.

Spinal cord

Following registration to the PAM50 spinal cord template (see Figure 2 animation 1) a cluster of activation representing the positive main effect of temperature was identified in the left dorsal horn (DH), in the C6 spinal segment (Figure 2B, assessed using permutation testing with a left C5/C6 mask, $P<0.05$, TFCE corrected). This represents activity in a population of spinal neurons that responded more strongly to noxious thermal stimulation. This $Spinal_{noci}$ cluster was somatotopically localised, given that the thermal stimuli were applied to the left forearm in the C6 dermatome (and its location was also confirmed without masking, Figure 2 Supplementary Figure 5). BOLD parameter estimates were extracted to investigate the activity of this $Spinal_{noci}$ cluster across the four experimental conditions and three drug sessions (Figure 2C & 2D). There was a positive corelation between the pain ratings and activity in the $Spinal_{noci}$ cluster across all subjects and

experimental conditions (Figure 2C). Accordingly in the placebo session, the pattern of BOLD signal change across conditions was similar to the pain scores (Figure 2A & 2D), and the response to a noxious stimulus was lower in the hard|high than easy|high condition, suggesting that the $Spinal_{noci}$ activity was modulated during attentional analgesia. A similar pattern was evident in the reboxetine condition however, this was not observed in the naltrexone arm consistent with the opioid antagonist-mediated blockade of attentional analgesia. Post hoc analysis of the differences in $Spinal_{noci}$ BOLD in the hard|high - easy|high conditions, although showing the same pattern of differences in the means, did not show a group level difference between drug sessions. This absence of evidence for attentional modulation of absolute BOLD signal differences may reflect large interindividual differences, low signal to noise in spinal cord fMRI data, or an inability to discriminate between excitatory or inhibitory contributions to measured signal (Figure 2 -Supplementary figure 2B).

Analysis of the task*temperature interaction revealed a second discrete spinal cluster ($Spinal_{int}$, Figure 2B). This was also located on the left side of the C6 segment but was slightly caudal, deeper and closer to the midline with respect to the $Spinal_{noci}$ cluster (with only marginal overlap). The location of this activity was again confirmed in an unmasked spinal analysis (Figure 2 Supplementary Figure 5). Extraction of BOLD parameter estimates from the $Spinal_{int}$ cluster in the placebo and reboxetine condition, showed an increased level of activity in the hard|high condition compared to the easy|high and hard|low conditions (Figure 2E). The $Spinal_{int}$ cluster showed significant activation in the hard|high condition in the placebo and reboxetine trials which was not evident in the presence of naltrexone (Figure 2 - Supplementary Figure 2C). This activity profile suggests this $Spinal_{int}$ cluster, potentially composed of spinal interneurons, plays a role in the modulation of nociception during the attentional analgesic effect.

Brainstem and whole brain

To identify the regions of the brainstem involved in mediating attentional analgesia and potentially interacting with the spinal cord, a similar pooled analysis strategy was employed. Activity in brainstem nuclei was investigated using permutation testing with a whole brainstem mask (significant results are reported for $P<0.05$, TFCE corrected), with subsequent attribution of signal to specific nuclei made through probabilistic masks (from

(Brooks et al., 2017), available from: https://osf.io/xqvb6/). Analysis of the main effect of temperature within a whole brainstem mask showed substantial clusters of activity in the midbrain (PAG) and medulla (RVM) with more discrete clusters in the dorsal pons bilaterally (LC) (Figure 3A, Figure 3 Supplementary Figure 1). In the main effect of task, the pattern of brainstem activation was more diffuse (Figure 3B, Figure 3 Supplementary Figure 1), but again included activation of the PAG, RVM and bilateral LC. Importantly for the mediation of attentional analgesia, no task*temperature interaction was observed within the brainstem (Figure 3 Supplementary Figure 1).

Whole-brain analysis of the main effect of temperature (mixed effects analysis, cluster forming threshold $Z > 3.1$, family wise error (FWE) corrected $P < 0.05$) showed activation in pain-associated regions such as primary somatosensory cortex, dorsal posterior insula, operculum, anterior cingulate cortex and cerebellum with larger clusters contralateral to the side of stimulation (i.e. right side of brain). A cluster in the medial pre-frontal cortex exhibited deactivation. (Figure 3B, Figure 3). For the main effect of task, bilateral activation was seen in attention and visual processing areas including lateral occipital cortex, anterior insular cortex and anterior cingulate cortex. Deactivation was observed in the cerebellum (Crus I), precuneus and lateral occipital cortex (superior division). (Figure 3B, Figure 3). No cluster in the whole brain analysis reached significance in the positive task*temperature interaction. Note that cluster thresholding does not permit inference on specific voxel locations (Woo et al., 2014), we report the full list of regions encompassed by each significant cluster (see Figure 3).

The distribution of these patterns of regional brain and brainstem activity were closely similar to those found in our previous studies of attentional analgesia (Brooks et al., 2017; Oliva et al., 2021a; Oliva et al., 2021b), with the difference that no area in the brain or brainstem showed a task*temperature interaction (unlike the spinal cord). Parameter maps for all subjects and conditions (in MNI space) for the main effect analyses of brain, brainstem and spinal cord are available from: https://osf.io/dtpr6/.

Attentional analgesia and effective network connectivity

Following identification of brain, brainstem and spinal cord regions active during the attentional analgesia paradigm, and in keeping with our pre-specified regions of interest, we

sought to investigate whether their connectivity was altered under the different experimental conditions and whether this was subject to specific neurotransmitter modulation. To determine the baseline evidence for the attentional analgesia network, we performed a generalised psychophysiological interaction (gPPI) analysis for the placebo condition alone within the *a priori* identified seed/target regions (after (Brooks et al., 2017; Oliva et al., 2021b) and based on previous human (Eippert et al., 2009b; Tracey et al., 2002) and animal studies (Fields, 2004; Ossipov et al., 2010) of descending control): ACC, PAG, right LC , RVM and cervical spinal cord (left C5/C6 mask).

The gPPI identified the following pairs of connections [seed-target] as being significantly modulated by our experimental conditions (Figure 4A, Figure 4 Supplementary Figure 1 & 2):

- main effect of temperature [PAG-rLC], [rLC-ACC], [rLC-RVM] and [RVM-spinal cord]
- main effect of task [RVM-rLC] and [PAG-ACC]
- task*temperature interaction [RVM-PAG], [RVM-rLC], and [RVM-spinal cord].

This pattern of network interactions has a number of common features shared with our previous analysis (Oliva et al., 2021b) including the task modulation of connectivity between PAG and ACC and the effect of the task*temperature interaction on connectivity between RVM and PAG. The new features were the important linkage between the spinal cord activity and RVM which is modulated by both temperature and the task*temperature interaction and also the influence of all conditions on communication between RVM and rLC.

Parameter estimates extracted from the connections modulated by task, revealed that the PAG-ACC, RVM-PAG, RVM-rLC, and RVM-Spinal cord connections were stronger in the hard|high versus the easy|high condition (Figure 4B), consistent with their potential roles in attentional analgesia.

Impact of neuromodulators on regional brain activations and network interactions

Having identified this group of regions, in a network spanning the length of the neuraxis, whose activity and connectivity correspond to aspects of the attentional analgesia paradigm

we examined whether naltrexone or reboxetine affected the regional BOLD activity or connectivity, comparing each drug against the placebo condition (using paired t-tests).

At the whole brain level, neither drug altered the activations seen for the main effect of temperature. Only the left anterior insula responded more strongly in the presence of Naltrexone for the main effect of task (Figure 3 Supplementary Figure 2), however this was not considered relevant to the analgesic effect as our behavioural findings showed no effect of naltrexone on task performance (Figure 2 Supplementary Figure 3B). In the brainstem, a stronger response to temperature was detected in the lower medulla in the presence of naltrexone compared to placebo (Figure 3 Supplementary Figure 2). There was no difference between naltrexone and placebo in the main effect of task in the brainstem. Similarly, no differences in either main effect were uncovered in the brainstem for the reboxetine versus placebo comparison.

The relative lack of effect of either drug on absolute BOLD signal changes provided little evidence for the localisation of their effects in either blocking attentional analgesia (naltrexone) or producing antinociception (reboxetine). However, it has previously been demonstrated that administration of opioidergic antagonists such as naloxone have measurable effects on neural dynamics assessed with fMRI e.g. (Eippert et al., 2009a). Therefore, we investigated the network of brain, brainstem and spinal regions that show effective connectivity changes associated with attentional analgesia (under the placebo condition) and explored whether these patterns were altered in the presence of reboxetine or naltrexone (paired t-tests versus placebo).

The administration of naltrexone, which abolished attentional analgesia behaviourally, significantly reduced the connection strength of RVM-spinal cord in the task*temperature interaction (Figure 5), indicating a role for opioids in this network interaction. The communication between ACC and PAG was also significantly weakened by both naltrexone and reboxetine, suggesting this connection to be modulated by both endogenous opioids and noradrenaline (Figure 5). The strength of the RVM-LC connection in the main effect of temperature was significantly diminished by reboxetine. None of the other connections in the network were altered significantly by the drugs compared to placebo.

Discussion

Using brain, brainstem and spinal cord fMRI we have been able to simultaneously measure the changes in neural activity during this attentional pain modulation study at all levels of the neuraxis during a randomised, placebo-controlled, crossover pharmacological study. This approach allowed unambiguous identification of the nociceptive signal at its site of entry in the dorsal horn and revealed that the task-driven cognitive reductions in pain perception echo the change in absolute BOLD signal at a spinal level. Remarkably the spinal imaging also identified a nearby cluster of neural activity that tracked the interaction between cognitive task and thermal stimulus. Analysis of effective connectivity between brain and brainstem regions and the spinal cord in a single acquisition allowed extension from previous findings (Brooks et al., 2017; Oliva et al., 2021a; Oliva et al., 2021b; Sprenger et al., 2012; Sprenger et al., 2015) to demonstrate causal changes mediating the interaction of pain and cognitive task including descending influences on the spinal dorsal horn. Naltrexone selectively blocked attentional analgesia and reduced connectivity between RVM and dorsal horn as well as between ACC and PAG. This provides evidence for opioid-dependent mechanisms in the descending pain modulatory pathway that is recruited to mediate the attentional modulation of pain.

The use of individually titrated noxious and innocuous stimuli from a thermode applied to the C6 dermatome of the medial forearm, allowed the identification of a somatotopic $Spinal_{noci}$ cluster in the main effect of temperature contrast in the dorsal horn of the C6 segment. This was strikingly similar to the pattern of activation noted in several previous focussed spinal imaging pain studies in humans (Brooks et al., 2012; Eippert et al., 2009b; Sprenger et al., 2012; Sprenger et al., 2015; Tinnermann et al., 2017) and non-human primates (Yang et al., 2015). The extracted absolute BOLD from the $Spinal_{noci}$ cluster was tightly correlated to the pain scores across the four experimental conditions and therefore the pattern of changes paralleled the changes in pain percept as it was modulated by task. This is similar to the seminal findings from electrophysiological recordings in non-human primates (Bushnell et al., 1984), which showed thermal stimulus evoked neural activity in the spinal nucleus of the trigeminal nerve to be altered by attentional focus. Further, it suggested that task related modulation of pain (Miron et al., 1989) could occur at the first relay point in the nociceptive transmission pathway. This finding of cognitive modulation of

nociceptive input was extended through human spinal fMRI by Sprenger and colleagues (2012), who in a second psychophysical experiment with naloxone provided evidence that the modulation of pain percept may involve opioids. We show that naltrexone attenuates spinal responses to attentional analgesia, which underly the behavioural differences between the high|hard and easy|hard conditions.

Uniquely, our 2x2 factorial study design enabled the identification of neural activity reading out the interaction between task and temperature which strikingly was only seen at a spinal level in a cluster located deep and medial to the $Spinal_{noci}$ cluster. The activity in this $Spinal_{int}$ cluster was highest in the high|hard condition (ie when the attentional analgesic effect is seen) and this activation was no longer significant in the presence of naltrexone. This may be consistent with the presence of a local interneuron population in the deeper dorsal horn that could influence the onward transmission of nociceptive information (Hughes and Todd, 2020; Koch et al., 2018). Such a circuit organisation is predicted by many animal models of pain regulation with the involvement of inhibitory interneurons that shape the incoming signals from the original gate theory of Melzack and Wall (Melzack and Wall, 1965) through to descending control (Millan, 2002). For example, opioids like enkephalin are released from such local spinal inter-neuronal circuits (Corder et al., 2018; Francois et al., 2017) and similarly descending noradrenergic projections exert their influence in part via inhibitory interneurons and an alpha1-adrenoceptor mechanism (Baba et al., 2000a; Baba et al., 2000b; Gassner et al., 2009; Yoshimura and Furue, 2006). As such the ability to resolve this $Spinal_{int}$ cluster may open a window into how such local interneuron pools are recruited to shape nociceptive transmission in humans according to cognitive context.

Since our goal was to explore the functional connections between brain, brainstem, and spinal cord, we opted to use a single acquisition, with identical imaging parameters (e.g. orientation of slices, voxel dimensions, point spread function) for the entire CNS. This differs from other approaches using different parameters for spinal and brain acquisitions in two fields of view ((Finsterbusch et al., 2012; Finsterbusch et al., 2013; Islam et al., 2019; Sprenger et al., 2015; Tinnermann et al., 2017) and reviewed in (Tinnermann et al., 2021)). Our choice was motivated by (i) the need to capture signal across the entire CNS region involved in the task (including the entire medulla), and (ii) that the use of different acquisition parameters for brain and spinal cord could be a confounding factor, particularly

for connectivity analyses, due to altered BOLD sensitivity and point-spread function for the separate image acquisitions. By taking advantage the z-shimming approach (Finsterbusch et al., 2012) and of the recently developed Spinal Cord Toolbox (De Leener et al., 2017), we have been able to detect significant BOLD signal changes in response to experimental manipulations, across the entire CNS.

A key objective of the study was to determine how the information regarding the attentional task demand could be conveyed to the spinal cord. Analysis of regional BOLD signal showed activity in both the main effect of task and of temperature in all three of the key brainstem sites PAG, RVM and LC with no interaction between task and temperature in the brainstem providing little indication as to which area might be mediating any analgesic effect (in line with previous (Oliva et al., 2021b)). However, an interaction effect was observed on the effective connectivity between RVM and dorsal horn, with coupling highest in the high|hard conditions. The importance of this descending connection to the attentional analgesic effect is emphasised by the effect of naltrexone which blocked both the modulation of RVM-spinal cord connectivity and attentional analgesia (a behavioural finding previously noted by Sprenger et al (2012)). This fits with the classic model of descending pain modulation that has been developed through decades of animal research (Fields, 2004; Ossipov et al., 2010) that is engaged in situations of fight or flight and also during appetitive behaviours like feeding and reproduction. Here we identify that the opioidergic system is also engaged moment by moment, in specific contexts, during a relatively simple cognitive tasks and uncover one of its loci of action in humans.

Analysis of effective connectivity also showed evidence for modulation of pathways from ACC to PAG and PAG to RVM by task and the interaction between task and temperature, respectively (in agreement with (Oliva et al., 2021b)). The communication between ACC and PAG was also disrupted by the opioid antagonist naltrexone. This is similar to the previous finding from studies of placebo analgesia where naloxone was shown to disrupt ACC-PAG communication which was also linked to the mediation of its analgesic effects (Eippert et al., 2009a) although behavioural findings of additive analgesia from concurrent placebo and attentional analgesia (Buhle et al., 2012) have been used to argue for distinct pathways of mediation. Activation of the analogous ACC-PAG pathway in rats has recently been shown to produce an analgesic effect mediated via an inhibition of activity at a spinal level

indicating that it indeed represents a component of the descending analgesic system (Drake et al., 2021). Interestingly this study also found that this system failed in a chronic neuropathic pain model. This provides evidence for top-down control of spinal nociception during distraction from pain, via the ACC-PAG-RVM-dorsal horn pathway. These findings suggest that the ACC primarily signals the high cognitive load associated with the task to the PAG, that recruits spinally-projecting cells in the RVM. Analgesia could be achieved through disinhibition of spinally-projecting OFF-cells (Heinricher et al., 1994; Lau and Vaughan, 2014; Roychowdhury and Fields, 1996), that inhibit dorsal horn neurons both directly via GABAergic and opioidergic projections to the primary afferents (Morgan et al., 2008; Zhang et al., 2015) and also indirectly via local inhibitory interneuron pools at a spinal level (Francois et al., 2017) reflected in reduced BOLD signal in the $Spinal_{noci}$ cluster and activation of the $Spinal_{int}$ pool.

Previous human imaging studies have provided evidence for a role of the locus coeruleus in attentional analgesia (Brooks et al., 2017; Oliva et al., 2021b). We replicate some of those findings in showing activity in the LC related to both task and thermal stimulus as well as interactions between the LC and RVM that were modulated by the interaction between task and temperature. However, we neither found evidence for an interaction between task and temperature nor for a correlation with analgesic effect in the LC that we reported in our previous studies (Brooks et al., 2017; Oliva et al., 2021b). We also could not demonstrate altered connectivity between the LC and the spinal cord during the paradigm as we anticipated given its known role in descending pain modulation (Hickey et al., 2014; Hirschberg et al., 2017; Llorca-Torralba et al., 2016; Millan, 2002; Oliva et al., 2021b; Ossipov et al., 2010). It is likely that the brainstem focussed slice prescription used previously is necessary for capturing sufficient signal from the LC, and that extending slice coverage to allow inclusion of the spinal cord compromised signal fidelity in this small brainstem nucleus. The noradrenergic manipulation with reboxetine did show a significant analgesic effect which was independent of task difficulty. This indicates that this dose of reboxetine is capable of altering baseline gain in the nociceptive system, but has no selective effect on attentional pain modulation. We performed a post hoc Bayesian paired t-test analysis contrasting reboxetine with placebo which showed moderate level of confidence in this null effect on attentional analgesia (Bayes Factor 6.8). Reboxetine also modulated a task-

dependent connection between ACC and PAG, though this did not appear to influence task performance and so its behavioural significance is uncertain. In interpreting these findings one potential explanation is that noradrenaline is not involved in attentional analgesia, however it could also be because of a ceiling effect where the reuptake inhibitor cannot increase the noradrenaline level any further during the attentional task. In this sense a noradrenergic antagonist experiment, similar to that used to examine the role of the opioids, would be ideal. However, selective alpha2-antagonists are not used clinically and even experimental agents like Yohimbine have a number of issues that would have confounded this study in that they cause anxiety, excitation and hypertension. Therefore, we conclude that were not able to provide any additional causal evidence to support a role of the LC in attentional analgesia, but this likely reflects a limitation of our approach and lack of good pharmacological tools to resolve the influence of this challenging target.

This combination of simultaneous whole CNS imaging with concurrent thermal stimulation and attentional task in the context of pharmacological manipulation, has enabled the identification of long-range network influences on spinal nociceptive processes and their neurochemistry. An important aspect of this approach is that it has enabled the linkage between a large body of fundamental pain neuroscience that focussed on primary afferent to spinal communication and brainstem interactions (nociception) which can be directly integrated to the findings of whole CNS human imaging. This also offers novel opportunities for translational studies to investigate mechanisms and demonstrate drug target engagement. The finding that it is the effective connectivity of these networks that is of importance in the mediation of the effect of attention and the influence of the opioid antagonist reflects recent observations from large scale studies relating psychological measures to functional connectivity (e.g. (Dubois et al., 2018)). In patient populations this focus on long range connectivity may help to differentiate between processes leading to augmented nociception and/or altered perception and control (e.g. in fibromyalgia (Oliva et al., 2021a)). Finally, we note that the location of the observed interaction between task and temperature indicates that cognitive tasks are integrated to act at the earliest level in the nociceptive transmission pathway introducing the novel concept of spinal psychology.

Methods

DATA ACQUISITION

Participants

Healthy volunteers were recruited through email and poster advertisement in the University of Bristol and were screened via self-report for their eligibility to participate. Exclusion criteria included any psychiatric disorder (including anxiety/depression), diagnosed chronic pain condition (e.g. fibromyalgia), left handedness, recent use of psychoactive compounds (e.g. recreational drugs or antidepressants) and standard MRI-safety exclusion criteria.

The study was approved by the University of Bristol Faculty of Science Human Research Ethics Committee (reference 23111759828). An initial power analysis was done to determine the sample size using the fmripower software (Mumford and Nichols, 2008). Using data from our previous study of attentional analgesia ((Brooks et al., 2017), main effect of task contrast in the periaqueductal grey matter mask) we designed the study to have an 80% power to detect an effect size of 0.425 (one sample t-test) in the PAG with an alpha of 0.05 requiring a cohort of 40 subjects. Of fifty-seven subjects screened, two were excluded for claustrophobia, three were excluded for regular or recent drug use (including recreational), and five were excluded due to intolerance of the thermal stimulus. This was defined as high pain score (≥ 8/10) for a temperature that should be non-nociceptive (<43 °C). In addition, six participants withdrew from the study as they were unable to attend for the full three visits. One participant had an adverse reaction (nausea) to a study drug (naltrexone) and dropped out of the study. One subject was excluded for being unable to perform the task correctly. Thirty-nine participants completed all three study visits (mean age 23.7, range [18 - 45] years, 18 females).

Calibration of temperature and task velocity

In the first screening/calibration visit, the participants were briefed on the experiment and gave written informed consent. The participants were familiarised with thermal stimulation by undergoing a modified version of quantitative sensory testing (QST) based on the DFNS protocol (Rolke et al., 2006). QST was performed using a Pathway device (MEDOC, Haifa,

Israel) with a contact ATS thermode of surface area 9cm^2 placed on the subject's left forearm (corresponding to the C6 dermatome). Subsequently, the CHEPS thermode (surface area 5.73cm^2) was used at the same site to deliver a 30 second hot stimulus, to determine the temperature to be used in the experimental visits. Each stimulus consisted of a plateau temperature of 36 to 45°C, and approximately thirty pseudorandomised "heat spikes" of 2, 3, or 4 degrees superimposed on the plateau, each lasting less than a second. This temperature profile was used in our previous studies (Brooks et al., 2017; Oliva et al., 2021a; Oliva et al., 2021b) to maintain painful perception, while at the same time avoiding sensitization and skin damage (Lautenbacher et al., 1995). Participants received a range of temperatures between 36 and 45°C, and were asked to rate the sensation they felt for each stimulus, on a scale from 0 (no pain) to 10 (the worst pain imaginable). The stimulus provoking a pain rating of 6 out of 10 at least 3 times in a row, was used for the "high" temperature stimulation in the experiment. If the participant only gave pain scores lower than 6 to all stimuli, then the maximum programmable plateau temperature of 45°C was used, but with higher temperature spikes of 3, 4 and 5 degrees above, reaching the highest temperature allowed for safety (50°C maximum).

The session also included a calibration of the rapid serial visual presentation (RSVP) task (Potter and Levy, 1969), where participants were asked to spot the number 5 among distractor characters. The task was repeated 16 times at different velocities (i.e. different inter-character intervals) in pseudorandom order, ranging from 32 to 256ms. To identify the optimal speed for the hard version of the RSVP task (defined as 70% of each subject's maximum d' score), the d' scores for the different velocities were plotted and the curve fit to a sigmoidal function, using a non-linear least squares fitting routine in Excel (Solver). Once parameterised, the target speed for 70% performance was recorded for subsequent use during the imaging session.

Imaging sessions

Following the screening/calibration session, participants returned for three imaging sessions, spaced at least a week apart. Participants underwent drug screening (questionnaire) and pregnancy testing. After eating a light snack, they were given either an inert placebo capsule, naltrexone (50mg) or reboxetine (4mg) according to a randomised

schedule. The dose of the opioid antagonist Naltrexone (50mg) was as per the British National Formulary (BNF) where it is licensed to prevent relapse in opioid or alcohol dependency. Naltrexone is well absorbed with high oral bioavailability and its levels in the serum peak after 1 hour with a half-life of between 8 and 12 hours (Verebey et al., 1976). Reboxetine is used for the treatment of depression, and we used the lowest dose recommended by the BNF (4mg). It has high oral bioavailability (~95%), serum levels peak at around 2 hours after oral administration and it has a half-life of 12 hours (Fleishaker, 2000). Both drugs have previously been used for imaging studies and these formed the basis for our choice of dosing and protocol timings. Oral naltrexone (50mg) produces 95% blockade of mu opioid receptor binding in the brain (assessed with Carfentanil PET, (Weerts et al., 2008)). Additionally, naltrexone (50mg) altered network activity in a pharmaco-fMRI study and was well tolerated (Morris et al., 2018). Oral reboxetine (4mg) has been used successfully in human volunteer studies of affective bias with fMRI neuroimaging (Harmer et al., 2003; Miskowiak et al., 2007). Harmer and colleagues reported an effect of the noradrenergic reuptake inhibitor on emotional processing but no effect on performance of a rapid serial visual presentation task.

All tablets were encased in identical gelatine capsules and dispensed in numbered bottles prepared by the hospital pharmacy (Bristol Royal Infirmary, University Hospitals Bristol and Weston NHS Foundation Trust). Neither the participant nor the investigator knew the identity of the drug which was allocated by a computer-generated randomised schedule. No subject reported being aware of whether they had received active drug or placebo (but the effectiveness of masking was not formally assessed post hoc after dosing).

One hour after drug dosing, calibration of the RSVP task was repeated (to control for any effect on performance). Before scanning, participants received the high thermal stimulus at their pre-determined temperature, which they rated verbally. If the rating was 6±1, the temperature was kept the same, otherwise it was adjusted accordingly (up or down). Neither reboxetine nor naltrexone caused a significant change in pain perception or task velocity during the calibration, as verified with paired t tests (placebo versus reboxetine and placebo versus naltrexone, see Figure 2 Supplementary Figure 3). On average, the plateau

temperature used for high temperature stimuli was 43.8± 1.25°C. The median inter-stimulus interval for the hard RSVP task was 48ms, range [32-96].

In the MRI scanner, participants performed the RSVP task at either difficulty level (easy or hard) whilst innocuous (low) or noxious (high) thermal stimuli were delivered concurrently to their left forearm. The four experimental conditions (*easy*|*high, hard*|*high, easy*|*low, hard*|*low*), were repeated four times each, in a pseudo-random order. The hard version (70% d' performance) of the task and the high (noxious) thermal stimulus were calibrated as described above. In the easy version of the task the inter-character presentation speed was always set at 192ms, except when a participant's hard task velocity of was equal or slower than 96ms, whereby the easy task was set to 256ms. The low (innocuous) thermal stimulus was always set to be a plateau of 36°C with spikes of 2, 3 and 4˚C above this baseline. Participants performed the task (identifying targets) and provided pain ratings 10 seconds after the end of each experimental block on a visual analogue scale (0-100), using a button box (Lumina) held in their dominant (right) hand.

Acquisition of functional images

Functional images were obtained with a 3T Siemens Skyra MRI scanner, and 64 channel receive-only head and neck coil. After acquisition of localiser images, a sagittal volumetric T1-weighted structural image of brain, brainstem and spinal cord was acquired using the MPRAGE pulse sequence, (TR = 2000ms, TE = 3.72ms, TI = 1000 ms, flip angle 9°, field of view (FoV) 320 mm, GRAPPA acceleration factor = 2) and 1.0mm isotropic resolution. Blood oxygenation level dependent (BOLD) functional data was acquired axially from the top of the brain to the intervertebral disc between the C6 and C7 vertebral bodies, with TR = 3000ms, TE = 39ms, GRAPPA acceleration factor = 2, flip angle 90°, FoV 170 mm, phase encoding direction P>>A, matrix size 96 by 96.

Slices were positioned perpendicular to the long axis of the cord for the C5-C6 spinal segments, whilst still maintaining whole brain coverage, and had an in-plane resolution of 1.77 x 1.77 mm and slice thickness of 4mm and a 40% gap between slices (increased to 45-50% in taller participants). To determine the optimal shim offset for each slice, calibration scans were acquired cycling through 15 shim offsets. For the caudal 20 slices covering from

spinal cord to medulla, manual inspection of images determined the optimal shim offset to be used for each subject (Finsterbusch et al., 2012). The remaining supraspinal slices were acquired with the first and higher order shim offsets determined using the scanner's automated routine. The ability of z-shimmed whole CNS imaging to adequately capture BOLD signal was assessed through pilot data examining the temporal signal to noise ratio (tSNR) across cord and brain, see Figure 1 Supplementary Figure 1.

During scanning, cardiac and respiratory processes were recorded using a finger pulse oximeter (Nonin 7500) and pneumatic respiratory bellows (Lafayette), respectively. These physiological signals and scanner triggers were recorded using an MP150 data acquisition unit (BIOPAC, Goleta, CA), and converted to text files for subsequent use during signal modelling.

DATA ANALYSIS

Analysis of pain scores

Pain scores recorded during the experiment were investigated collectively for the three visits using a three-way ANOVA in Prism version 8 for Windows (GraphPad Software, La Jolla, California). Any significant interaction was further investigated with two separate three-way ANOVAs (placebo versus naltrexone and placebo versus reboxetine). Finally, each drug condition was analysed individually with three separate two-way ANOVAs. Two-tailed post-hoc tests were used to further investigate any interactions.

Pre-processing of functional data and single-subject analysis

Functional data were divided into spinal cord and brain/brainstem, by splitting at the top of the odontoid process (dens) of the 2nd cervical vertebra. The resulting two sets of images underwent separate, optimised, pre-processing pipelines.

Spinal cord data was motion corrected with AFNI 2dImReg (Cox, 1996), registering all time points to the temporal mean. Data was smoothed with an in-plane 2D Gaussian smoothing kernel of 2mm x 2mm FWHM, using an in-house generated script. The Spinal Cord Toolbox (SCT, v4.1.1) was then used to create a 25mm diameter cylindrical mask around the entire cord to crop the functional data. The SCT was also used to segment the cord from the

cerebrospinal fluid (CSF) and register functional images to the PAM50 template (De Leener et al., 2018). Manual intervention was necessary to ensure accurate cord segmentation on EPI data. The registration pipeline included two steps: (1) registration of each subject's T1-weighted structural scan to the PAM50 T1-weighted template, (2) registration of acquired functional images to PAM50 template (T2*-weighted) using the output from step 1 as an initial warping. The inverse warping fields generated by this process were also used to transform the PAM50 CSF mask to subject space (Figure 2 Supplementary Figure 4 and Animation 1). The mask was then used to create a CSF regressor for use during correction for physiological noise during first level FEAT analysis (part of FSL, (Jenkinson et al., 2012)).

Brain functional data was pre-processed and analysed in FEAT. Pre-processing included smoothing with a 6mm Gaussian kernel, and motion correction with MCFLIRT (Jenkinson et al., 2002). Functional data was unwarped with a fieldmap using FUGUE (Jenkinson, 2003), then co-registered to the subject's T1-weighted structural scan using boundary-based registration (Greve and Fischl, 2009). Structural scans were registered to the 2mm MNI template using a combination of linear (FLIRT, (Jenkinson and Smith, 2001)) and non-linear (FNIRT, (Andersson et al., 2007)) registration with 5mm warp resolution.

Physiological noise correction was conducted for the brain and spinal cord (Brooks et al., 2008; Harvey et al., 2008) within FEAT, and as recommended for use in PPI analyses (Barton et al., 2015). Cardiac and respiratory phases were determined using a physiological noise model (PNM, part of FSL), and slice specific regressors determined for the entire CNS coverage. Subsequently these regressors (which are 4D images) were split at the level of the odontoid process, to be used separately for brain and spinal cord physiological noise correction. For the brain data the PNM consisted of 32 regressors, with the addition of a CSF regressor for the spinal cord, giving a total of 33 regressors for this region.

All functional images were analysed using a general linear model (GLM) in FEAT with high-pass temporal filtering (cut-off 90s) and pre-whitening using FILM (Woolrich et al., 2001). The model included a regressor for each of the experimental conditions (*easy*|*high*, *hard*|*high*, *easy*|*low*, *hard*|*low*), plus regressors of no interest (task instructions, rating periods), and their temporal derivatives. Motion parameters and physiological regressors

were also included in the model to help explain signal variation due to bulk movement and physiological noise. The experimental regressors of interest were used to build the following planned statistical contrasts: positive and negative main effect of temperature (high temperature conditions versus low temperature conditions and vice versa), positive and negative main effect of task (hard task conditions versus easy task conditions and vice versa), and positive and negative interactions.

Activity within the cerebrum was assessed using conventional whole-brain cluster-based thresholding and mixed-effects modelling, based on recent recommendations (Eklund et al., 2016). However, such an approach would not have been appropriate for the small, non-spherical nuclei within the brainstem and laminar arrangement of the spinal cord dorsal horn, which will typically have a larger rostro-caudal extent. Here we chose to use probabilistic anatomical masks (from (Brooks et al., 2017) and available from https://osf.io/xqvb6/ and (De Leener et al., 2017)) to restrict analysis to specific regions, along with permutation testing to assess significance levels with threshold free cluster enhancement (TFCE) (Smith and Nichols, 2009).

Group analysis

We used a conservative approach to investigate differences in CNS activity in main effects and interactions due to administration of reboxetine or naltrexone. All first-level analyses, single group averages and pooled analyses were performed with the experimenter masked to the study visit (i.e. drug session). An initial analysis examined the brain, brainstem, and spinal cord activation in the planned contrasts (main effects of temperature, task, and their interaction) across all visits i.e. a "pooled" analysis. Individual subjects' data were averaged using a within-subject "group" model (treating variance between sessions as a random effect), and resultant outputs averaged (across subjects) using a mixed effects model. This allowed the generation of functional masks, to use for investigation of differences between drug conditions.

Generalised psychophysiological interaction (gPPI) analysis (McLaren et al., 2012) was used to assess effective connectivity changes between brain, brainstem, and spinal cord during the attentional analgesia experiment. The list of regions to be investigated were specified *a*

priori on the basis of our previous study (Oliva et al., 2021b), and included the ACC, PAG, LC and RVM – to which was added the left side of the spinal cord at the C5/C6 vertebral level. Following partial unblinding to drug, an initial analysis was performed for the placebo visit. This analysis strategy, which examined connectivity between CNS regions identified in the pooled data and previously (Brooks et al., 2017; Oliva et al., 2021b), was initially limited to examination of the placebo data and largely replicated our earlier findings (Oliva et al., 2021b). By identifying those connections that are normally active during attentional analgesia, we could then test whether they are subject to specific neurotransmitter modulation. This involved partial-unmasking to the remaining two conditions (information on the specific drug used was withheld), so paired t-tests could be performed between the connections of interest. Finally, after the analysis was completed the full unmasking was allowed for the purpose of interpretation of paired differences between conditions.

Pooled analysis – spinal cord

For each subject, parameter maps estimated for each contrast and each visit (i.e. drug session), were registered to the PAM50 template with SCT. Each contrast was then averaged across visits using a within-subject ordinary least squares (OLS) model using FLAME (part of FSL) from command line. The resulting average contrasts (registered to the PAM50 template) were each concatenated across subjects (i.e. each contrast had 39 samples). These were then investigated with a one-sample t-test in RANDOMISE, using a left C5-6 vertebral mask, based on the probabilistic atlas from the SCT. The choice to use a relatively large vertebral level mask, rather than a more focussed grey matter mask, was based on consideration of (1) the voxel size of our fMRI data compared to the high-resolution data (0.5mm) used to define probabilistic grey matter masks in SCT, and (2) to allow for inter-subject differences in segmental representation of the stimulation site on the left forearm. It should be noted that by using larger masks we effectively decreased our sensitivity to detect activation, due to the more punitive multiple comparison correction. Results are reported with threshold free cluster enhancement (TFCE) $P < 0.05$ corrected for multiple comparisons. Significant regions of activation from this pooled analysis were used to generate masks for subsequent comparison between conditions, using paired t-tests.

Pooled analysis – brainstem

Similar to the spinal cord, for each subject, parameter maps from the brainstem for each planned contrast and visit were averaged with an OLS model in FEAT software. The resulting average was the input to a between-subjects, mixed effects, one-sample t-test in FEAT. Subsequently, group activations for each of the six contrasts were investigated with permutation testing in RANDOMISE, using a probabilistic mask of the brainstem taken from the Harvard-Oxford subcortical atlas (threshold set to P=0.5). Results are reported with TFCE correction and $P < 0.05$. Significant regions of activity were binarized and used as a functional mask for the between conditions comparison.

Pooled analysis – brain

Brain data was averaged and analysed with the same FEAT analyses that were applied in the brainstem. Following within subject averaging, group activity was assessed with a mixed effects two-tailed one sample t-test at the whole-brain level, with results reported for cluster forming threshold of $Z > 3.1$, and corrected cluster significance of $P < 0.05$. This produced maps of activity (one per planned contrast) that were then binarized to produce masks that were used in follow up paired t-tests.

Within subject comparison – paired tests

Paired t tests were performed to resolve potential changes in activity in reboxetine versus placebo and naltrexone versus placebo, separately. Design and contrast files for input in RANDOMISE were built in FEAT. A group file with appropriately defined exchangeability blocks was additionally defined. Permutation testing in RANDOMISE was used to assess group level differences between placebo and the two drugs, separately for brain, brainstem, and spinal cord. The investigation was restricted to the functional masks derived from the main effect analysis for each contrast.

Effective connectivity analysis (gPPI)

For connectivity analysis, functional data for brain, brainstem and spinal cord were pre-processed as previously described (Oliva et al., 2021b). To restrict analysis to connections typically observed during attentional analgesia, we initially estimated the connection pattern for the placebo session, then within this network tested for differences in the other drug conditions. To achieve this goal, placebo data were first analysed for main

effects/interaction with the simple (non-gPPI) analysis to define the pattern of BOLD activity. Subsequently, time series extraction was restricted to anatomical regions/contrasts identified previously (Oliva et al., 2021b), and a left sided C5/C6 spinal mask which was used to determine spinal cord activation (derived from the spinal cord toolbox, (De Leener et al., 2017)). Physiological time-series were extracted from the voxel of greatest significance identified in the analysis of the placebo session, within the prespecified anatomical regions. In particular, time series were extracted from the peak voxel responding to the main effect of temperature in the RVM and spinal cord, the main effect of task in the ACC, PAG and LC, and the task * temperature interaction in the spinal cord (see Figure 4 Supplementary Figure 1 & 2).

For gPPI, physiological time-series were included in a GLM that also included the same regressors present in the first level main effects analysis i.e. regressors for the experimental conditions and all nuisance regressors (rating period, instruction, PNM, movement parameters). Interaction regressors were then built by multiplying the physiological time-series by each of the experimental regressors, and the planned contrasts constructed (e.g. positive main effect of task). Slice timing correction was not used for this connectivity analysis, as (1) there is no clear recommendation for its use (Harrison et al., 2017; McLaren et al., 2012; O'Reilly et al., 2012) (2) it was omitted in a similar cortico-spinal fMRI study (Tinnermann et al., 2017) and (3) to be consistent with our previous study (Oliva et al., 2021b). Apart from systematically varying the input physiological timeseries corresponding to different seed regions, models used for estimating connectivity for brain and spinal cord seeds were otherwise identical. Estimates of effective connectivity for the group were obtained with permutation testing with RANDOMISE, using as targets the same ROI masks used for time-series extraction. For example, a gPPI analysis with an RVM seed timeseries (taken from the region responding during the main effect of temperature), examined connectivity to brain/brainstem and spinal cord with PAG, LC, ACC, and left C5-6 vertebral masks. To test whether drug administration altered connectivity during attentional analgesia, the significant connections detected in the placebo session were examined for differences in the other drug conditions i.e. the *same masks* were used for time-series extraction for gPPI analysis of the naltrexone/reboxetine conditions. At the group level, two-tailed paired t-tests were used to detect differences with RANDOMSISE (TFCE, $P<0.05$)

between placebo and naltrexone, and between placebo and reboxetine visits, as described above.

Competing interests:

AEP declares that he has unrelated research funding for a collaboration with Eli Lilly and is on the advisory board for Lateral Pharma for an unrelated study. The other authors declare that they have no competing interests.

Acknowledgements

The authors would like to thank Aileen Wilson (Lead Research Radiographer, CRiCBristol) for her support in running experiments, and the subjects who kindly agreed to take part. This research was funded in whole, or in part, by the Wellcome Trust [203963/Z/16/Z; and 088373/Z/09/A] and Medical Research Council [MR/N026969/1]. For the purpose of Open Access, the author has applied a CC BY public copyright licence to any Author Accepted Manuscript version arising from this submission.

References

Andersson, J.L.R., Jenkinson, M., and Smith, S. (2007). Non-linear registration aka Spatial normalisation FMRIB Technial Report TR07JA2.

Aston-Jones, G., and Cohen, J.D. (2005). An integrative theory of locus coeruleus-norepinephrine function: adaptive gain and optimal performance. Annu Rev Neurosci 28, 403-450.

Baba, H., Goldstein, P.A., Okamoto, M., Kohno, T., Ataka, T., Yoshimura, M., and Shimoji, K. (2000a). Norepinephrine facilitates inhibitory transmission in substantia gelatinosa of adult rat spinal cord (part 2): effects on somatodendritic sites of GABAergic neurons. Anesthesiology 92, 485-492.

Baba, H., Shimoji, K., and Yoshimura, M. (2000b). Norepinephrine facilitates inhibitory transmission in substantia gelatinosa of adult rat spinal cord (part 1): effects on axon terminals of GABAergic and glycinergic neurons. Anesthesiology 92, 473-484.

Bantick, S.J., Wise, R.G., Ploghaus, A., Clare, S., Smith, S.M., and Tracey, I. (2002). Imaging how attention modulates pain in humans using functional MRI. Brain 125, 310-319.

Barton, M., Marecek, R., Rektor, I., Filip, P., Janousova, E., and Mikl, M. (2015). Sensitivity of PPI analysis to differences in noise reduction strategies. J Neurosci Methods 253, 218-232.

Benedetti, F., and Piedimonte, A. (2019). The neurobiological underpinnings of placebo and nocebo effects. Semin Arthritis Rheum 49, S18-S21.

Brooks, J.C., Beckmann, C.F., Miller, K.L., Wise, R.G., Porro, C.A., Tracey, I., and Jenkinson, M. (2008). Physiological noise modelling for spinal functional magnetic resonance imaging studies. Neuroimage 39, 680-692.

Brooks, J.C., Davies, W.E., and Pickering, A.E. (2017). Resolving the Brainstem Contributions to Attentional Analgesia. J Neurosci 37, 2279-2291.

Brooks, J.C., Kong, Y., Lee, M.C., Warnaby, C.E., Wanigasekera, V., Jenkinson, M., and Tracey, I. (2012). Stimulus Site and Modality Dependence of Functional Activity within the Human Spinal Cord. J Neurosci 32, 6231-6239.

Buhle, J.T., Stevens, B.L., Friedman, J.J., and Wager, T.D. (2012). Distraction and placebo: two separate routes to pain control. Psychol Sci 23, 246-253.

Bushnell, M.C., Ceko, M., and Low, L.A. (2013). Cognitive and emotional control of pain and its disruption in chronic pain. Nat Rev Neurosci 14, 502-511.

Bushnell, M.C., Duncan, G.H., Dubner, R., and He, L.F. (1984). Activity of trigeminothalamic neurons in medullary dorsal horn of awake monkeys trained in a thermal discrimination task. J Neurophysiol 52, 170-187.

Bussing, A., Ostermann, T., Neugebauer, E.A., and Heusser, P. (2010). Adaptive coping strategies in patients with chronic pain conditions and their interpretation of disease. BMC Public Health 10, 507.

Cohen-Adad, J., Gauthier, C.J., Brooks, J.C., Slessarev, M., Han, J., Fisher, J.A., Rossignol, S., and Hoge, R.D. (2010). BOLD signal responses to controlled hypercapnia in human spinal cord. Neuroimage 50, 1074-1084.

Corder, G., Castro, D.C., Bruchas, M.R., and Scherrer, G. (2018). Endogenous and Exogenous Opioids in Pain. Annu Rev Neurosci 41, 453-473.

Cox, R.W. (1996). AFNI: software for analysis and visualization of functional magnetic resonance neuroimages. Comput Biomed Res 29, 162-173.

781 Crombez, G., Eccleston, C., Van den Broeck, A., Goubert, L., and Van Houdenhove, B. (2004).
782 Hypervigilance to pain in fibromyalgia: the mediating role of pain intensity and catastrophic
783 thinking about pain. The Clinical journal of pain 20, 98-102.
784 De Felice, M., Sanoja, R., Wang, R., Vera-Portocarrero, L., Oyarzo, J., King, T., Ossipov, M.H.,
785 Vanderah, T.W., Lai, J., Dussor, G.O*., et al.* (2011). Engagement of descending inhibition
786 from the rostral ventromedial medulla protects against chronic neuropathic pain. Pain 152,
787 2701-2709.
788 De Leener, B., Fonov, V.S., Collins, D.L., Callot, V., Stikov, N., and Cohen-Adad, J. (2018).
789 PAM50: Unbiased multimodal template of the brainstem and spinal cord aligned with the
790 ICBM152 space. Neuroimage 165, 170-179.
791 De Leener, B., Levy, S., Dupont, S.M., Fonov, V.S., Stikov, N., Louis Collins, D., Callot, V., and
792 Cohen-Adad, J. (2017). SCT: Spinal Cord Toolbox, an open-source software for processing
793 spinal cord MRI data. Neuroimage 145, 24-43.
794 Drake, R.A., Steel, K.A., Apps, R., Lumb, B.M., and Pickering, A.E. (2021). Loss of cortical
795 control over the descending pain modulatory system determines the development of the
796 neuropathic pain state in rats. Elife 10.
797 Dubois, J., Galdi, P., Paul, L.K., and Adolphs, R. (2018). A distributed brain network predicts
798 general intelligence from resting-state human neuroimaging data. Philos Trans R Soc Lond B
799 Biol Sci 373.
800 Duval, T., McNab, J.A., Setsompop, K., Witzel, T., Schneider, T., Huang, S.Y., Keil, B., Klawiter,
801 E.C., Wald, L.L., and Cohen-Adad, J. (2015). In vivo mapping of human spinal cord
802 microstructure at 300mT/m. Neuroimage 118, 494-507.
803 Eccleston, C., and Crombez, G. (1999). Pain demands attention: a cognitive-affective model
804 of the interruptive function of pain. Psychological bulletin 125, 356-366.
805 Eippert, F., Bingel, U., Schoell, E.D., Yacubian, J., Klinger, R., Lorenz, J., and Buchel, C.
806 (2009a). Activation of the opioidergic descending pain control system underlies placebo
807 analgesia. Neuron 63, 533-543.
808 Eippert, F., Finsterbusch, J., Bingel, U., and Buchel, C. (2009b). Direct evidence for spinal
809 cord involvement in placebo analgesia. Science 326, 404.
810 Eklund, A., Nichols, T.E., and Knutsson, H. (2016). Cluster failure: Why fMRI inferences for
811 spatial extent have inflated false-positive rates. Proc Natl Acad Sci U S A 113, 7900-7905.
812 Erpelding, N., and Davis, K.D. (2013). Neural underpinnings of behavioural strategies that
813 prioritize either cognitive task performance or pain. Pain 154, 2060-2071.
814 Fields, H. (2004). State-dependent opioid control of pain. Nat Rev Neurosci 5, 565-575.
815 Fields, H.L., and Basbaum, A.I. (1978). Brainstem Control of Spinal P Ain -Transmission
816 Neurons. Ann Rev Physiol 40, 217-248.
817 Finsterbusch, J., Eippert, F., and Buchel, C. (2012). Single, slice-specific z-shim gradient
818 pulses improve T2*-weighted imaging of the spinal cord. Neuroimage 59, 2307-2315.
819 Finsterbusch, J., Sprenger, C., and Buchel, C. (2013). Combined T2*-weighted measurements
820 of the human brain and cervical spinal cord with a dynamic shim update. Neuroimage 79,
821 153-161.
822 Fleishaker, J.C. (2000). Clinical pharmacokinetics of reboxetine, a selective norepinephrine
823 reuptake inhibitor for the treatment of patients with depression. Clin Pharmacokinet 39,
824 413-427.
825 Francois, A., Low, S.A., Sypek, E.I., Christensen, A.J., Sotoudeh, C., Beier, K.T., Ramakrishnan,
826 C., Ritola, K.D., Sharif-Naeini, R., Deisseroth, K*., et al.* (2017). A Brainstem-Spinal Cord

827 Inhibitory Circuit for Mechanical Pain Modulation by GABA and Enkephalins. Neuron 93,
828 822-839 e826.
829 Gassner, M., Ruscheweyh, R., and Sandkuhler, J. (2009). Direct excitation of spinal
830 GABAergic interneurons by noradrenaline. Pain 145, 204-210.
831 Gracely, R.H., Geisser, M.E., Giesecke, T., Grant, M.A., Petzke, F., Williams, D.A., and Clauw,
832 D.J. (2004). Pain catastrophizing and neural responses to pain among persons with
833 fibromyalgia. Brain 127, 835-843.
834 Greve, D.N., and Fischl, B. (2009). Accurate and robust brain image alignment using
835 boundary-based registration. Neuroimage 48, 63-72.
836 Harmer, C.J., Hill, S.A., Taylor, M.J., Cowen, P.J., and Goodwin, G.M. (2003). Toward a
837 neuropsychological theory of antidepressant drug action: increase in positive emotional bias
838 after potentiation of norepinephrine activity. Am J Psychiatry 160, 990-992.
839 Harrison, T.M., McLaren, D.G., Moody, T.D., Feusner, J.D., and Bookheimer, S.Y. (2017).
840 Generalized Psychophysiological Interaction (PPI) Analysis of Memory Related Connectivity
841 in Individuals at Genetic Risk for Alzheimer's Disease. J Vis Exp.
842 Harvey, A.K., Pattinson, K.T., Brooks, J.C., Mayhew, S.D., Jenkinson, M., and Wise, R.G.
843 (2008). Brainstem functional magnetic resonance imaging: disentangling signal from
844 physiological noise. J Magn Reson Imaging 28, 1337-1344.
845 Heinricher, M.M., Morgan, M.M., Tortorici, V., and Fields, H.L. (1994). Disinhibition of off-
846 cells and antinociception produced by an opioid action within the rostral ventromedial
847 medulla. Neuroscience 63, 279-288.
848 Hickey, L., Li, Y., Fyson, S.J., Watson, T.C., Perrins, R., Hewinson, J., Teschemacher, A.G.,
849 Furue, H., Lumb, B.M., and Pickering, A.E. (2014). Optoactivation of locus ceruleus neurons
850 evokes bidirectional changes in thermal nociception in rats. J Neurosci 34, 4148-4160.
851 Hirschberg, S., Li, Y., Randall, A., Kremer, E.J., and Pickering, A.E. (2017). Functional
852 dichotomy in spinal- vs prefrontal-projecting locus coeruleus modules splits descending
853 noradrenergic analgesia from ascending aversion and anxiety in rats. Elife 6, e29808-
854 e29808.
855 Hughes, D.I., and Todd, A.J. (2020). Central Nervous System Targets: Inhibitory Interneurons
856 in the Spinal Cord. Neurotherapeutics 17, 874-885.
857 Hughes, S., Hickey, L., Donaldson, L.F., Lumb, B.M., and Pickering, A.E. (2015). Intrathecal
858 reboxetine suppresses evoked and ongoing neuropathic pain behaviours by restoring spinal
859 noradrenergic inhibitory tone. Pain 156, 328-334.
860 Islam, H., Law, C.S.W., Weber, K.A., Mackey, S.C., and Glover, G.H. (2019). Dynamic per slice
861 shimming for simultaneous brain and spinal cord fMRI. Magn Reson Med 81, 825-838.
862 Jenkinson, M. (2003). Fast, automated, N-dimensional phase-unwrapping algorithm.
863 Magnetic resonance in medicine : official journal of the Society of Magnetic Resonance in
864 Medicine / Society of Magnetic Resonance in Medicine 49, 193-197.
865 Jenkinson, M., Bannister, P., Brady, M., and Smith, S. (2002). Improved optimization for the
866 robust and accurate linear registration and motion correction of brain images. Neuroimage
867 17, 825-841.
868 Jenkinson, M., Beckmann, C.F., Behrens, T.E., Woolrich, M.W., and Smith, S.M. (2012). Fsl.
869 Neuroimage 62, 782-790.
870 Jenkinson, M., and Smith, S. (2001). A global optimisation method for robust affine
871 registration of brain images. Med Image Anal 5, 143-156.
872 Koch, S.C., Acton, D., and Goulding, M. (2018). Spinal Circuits for Touch, Pain, and Itch. Annu
873 Rev Physiol 80, 189-217.

874 Kong, Y., Jenkinson, M., Andersson, J., Tracey, I., and Brooks, J.C. (2012). Assessment of
875 physiological noise modelling methods for functional imaging of the spinal cord.
876 Neuroimage 60, 1538-1549.
877 Lakens, D. (2017). Equivalence Tests: A Practical Primer for t Tests, Correlations, and Meta-
878 Analyses. Soc Psychol Personal Sci 8, 355-362.
879 Lau, B.K., and Vaughan, C.W. (2014). Descending modulation of pain: the GABA disinhibition
880 hypothesis of analgesia. Curr Opin Neurobiol 29, 159-164.
881 Lautenbacher, S., Roscher, S., and Strian, F. (1995). Tonic pain evoked by pulsating heat:
882 temporal summation mechanisms and perceptual qualities. Somatosens Mot Res 12, 59-70.
883 Llorca-Torralba, M., Borges, G., Neto, F., Mico, J.A., and Berrocoso, E. (2016). Noradrenergic
884 Locus Coeruleus pathways in pain modulation. Neuroscience 338, 93-113.
885 Lorenz, J., Minoshima, S., and Casey, K.L. (2003). Keeping pain out of mind: the role of the
886 dorsolateral prefrontal cortex in pain modulation. Brain 126, 1079-1091.
887 McLaren, D.G., Ries, M.L., Xu, G., and Johnson, S.C. (2012). A generalized form of context-
888 dependent psychophysiological interactions (gPPI): a comparison to standard approaches.
889 Neuroimage 61, 1277-1286.
890 Melzack, R., and Wall, P.D. (1965). Pain mechanisms: a new theory. Science 150, 971-979.
891 Millan, M.J. (2002). Descending control of pain. Prog Neurobiol 66, 355-474.
892 Miron, D., Duncan, G.H., and Bushnell, M.C. (1989). Effects of attention on the intensity and
893 unpleasantness of thermal pain. Pain 39, 345-352.
894 Miskowiak, K., Papadatou-Pastou, M., Cowen, P.J., Goodwin, G.M., Norbury, R., and Harmer,
895 C.J. (2007). Single dose antidepressant administration modulates the neural processing of
896 self-referent personality trait words. Neuroimage 37, 904-911.
897 Morgan, M.M., Whittier, K.L., Hegarty, D.M., and Aicher, S.A. (2008). Periaqueductal gray
898 neurons project to spinally projecting GABAergic neurons in the rostral ventromedial
899 medulla. Pain 140, 376-386.
900 Morris, L.S., Baek, K., Tait, R., Elliott, R., Ersche, K.D., Flechais, R., McGonigle, J., Murphy, A.,
901 Nestor, L.J., Orban, C.*, et al.* (2018). Naltrexone ameliorates functional network
902 abnormalities in alcohol-dependent individuals. Addict Biol 23, 425-436.
903 Mumford, J.A., and Nichols, T.E. (2008). Power calculation for group fMRI studies accounting
904 for arbitrary design and temporal autocorrelation. Neuroimage 39, 261-268.
905 O'Reilly, J.X., Woolrich, M.W., Behrens, T.E., Smith, S.M., and Johansen-Berg, H. (2012).
906 Tools of the trade: psychophysiological interactions and functional connectivity. Soc Cogn
907 Affect Neurosci 7, 604-609.
908 Oliva, V., Gregory, R., Brooks, J.C.W., and Pickering, A.E. (2021a). Central pain modulatory
909 mechanisms of attentional analgesia are preserved in fibromyalgia. Pain in Press.
910 Oliva, V., Gregory, R., Davies, W.E., Harrison, L., Moran, R., Pickering, A.E., and Brooks,
911 J.C.W. (2021b). Parallel cortical-brainstem pathways to attentional analgesia. Neuroimage
912 226, 117548.
913 Ossipov, M.H., Dussor, G.O., and Porreca, F. (2010). Central modulation of pain. J Clin Invest
914 120, 3779-3787.
915 Petrovic, P., Kalso, E., Petersson, K.M., and Ingvar, M. (2002). Placebo and opioid analgesia--
916 imaging a shared neuronal network. Science 295, 1737-1740.
917 Peyron, R., Laurent, B., and Garcia-Larrea, L. (2000). Functional imaging of brain responses
918 to pain. A review and meta-analysis (2000). Neurophysiol Clin 30, 263-288.
919 Potter, M.C., and Levy, E.I. (1969). Recognition memory for a rapid sequence of pictures. J
920 Exp Psychol 81, 10-15.

Rolke, R., Baron, R., Maier, C., Tolle, T.R., Treede, R.D., Beyer, A., Binder, A., Birbaumer, N., Birklein, F., Botefur, I.C.*, et al.* (2006). Quantitative sensory testing in the German Research Network on Neuropathic Pain (DFNS): standardized protocol and reference values. Pain 123, 231-243.

Roychowdhury, S.M., and Fields, H.L. (1996). Endogenous opioids acting at a medullary μ-opioid receptor contribute to the behavioral antinociception produced by GABA antagonism in the midbrain periaqueductal gray. Neuroscience 74, 863-872.

Sara, S.J., and Bouret, S. (2012). Orienting and reorienting: the locus coeruleus mediates cognition through arousal. Neuron 76, 130-141.

Smith, S.M., and Nichols, T.E. (2009). Threshold-free cluster enhancement: addressing problems of smoothing, threshold dependence and localisation in cluster inference. Neuroimage 44, 83-98.

Sprenger, C., Eippert, F., Finsterbusch, J., Bingel, U., Rose, M., and Buchel, C. (2012). Attention modulates spinal cord responses to pain. Curr Biol 22, 1019-1022.

Sprenger, C., Finsterbusch, J., and Buchel, C. (2015). Spinal cord-midbrain functional connectivity is related to perceived pain intensity: a combined spino-cortical FMRI study. J Neurosci 35, 4248-4257.

Tinnermann, A., Buchel, C., and Cohen-Adad, J. (2021). Cortico-spinal imaging to study pain. Neuroimage 224, 117439.

Tinnermann, A., Geuter, S., Sprenger, C., Finsterbusch, J., and Buchel, C. (2017). Interactions between brain and spinal cord mediate value effects in nocebo hyperalgesia. Science 358, 105-108.

Tracey, I., Ploghaus, A., Gati, J.S., Clare, S., Smith, S., Menon, R.S., and Matthews, P.M. (2002). Imaging attentional modulation of pain in the periaqueductal gray in humans. J Neurosci 22, 2748-2752.

Valet, M., Sprenger, T., Boecker, H., Willoch, F., Rummeny, E., Conrad, B., Erhard, P., and Tolle, T.R. (2004). Distraction modulates connectivity of the cingulo-frontal cortex and the midbrain during pain--an fMRI analysis. Pain 109, 399-408.

Verebey, K., Volavka, J., Mule, S.J., and Resnick, R.B. (1976). Naltrexone: disposition, metabolism, and effects after acute and chronic dosing. Clin Pharmacol Ther 20, 315-328.

Wager, T.D., and Atlas, L.Y. (2015). The neuroscience of placebo effects: connecting context, learning and health. Nat Rev Neurosci 16, 403-418.

Weerts, E.M., Kim, Y.K., Wand, G.S., Dannals, R.F., Lee, J.S., Frost, J.J., and McCaul, M.E. (2008). Differences in delta- and mu-opioid receptor blockade measured by positron emission tomography in naltrexone-treated recently abstinent alcohol-dependent subjects. Neuropsychopharmacology : official publication of the American College of Neuropsychopharmacology 33, 653-665.

Woo, C.W., Krishnan, A., and Wager, T.D. (2014). Cluster-extent based thresholding in fMRI analyses: pitfalls and recommendations. Neuroimage 91, 412-419.

Woolrich, M.W., Ripley, B.D., Brady, M., and Smith, S.M. (2001). Temporal autocorrelation in univariate linear modeling of FMRI data. Neuroimage 14, 1370-1386.

Yang, P.F., Wang, F., and Chen, L.M. (2015). Differential fMRI Activation Patterns to Noxious Heat and Tactile Stimuli in the Primate Spinal Cord. J Neurosci 35, 10493-10502.

Yoshimura, M., and Furue, H. (2006). Mechanisms for the anti-nociceptive actions of the descending noradrenergic and serotonergic systems in the spinal cord. J Pharmacol Sci 101, 107-117.

967 Zhang, Y., Zhao, S., Rodriguez, E., Takatoh, J., Han, B.X., Zhou, X., and Wang, F. (2015).
968 Identifying local and descending inputs for primary sensory neurons. J Clin Invest 125, 3782-
969 3794.

970

971
972

Figure Legends

Figure 1: Experimental design. A total of 39 healthy subjects had thermal stimulation (to left forearm) while performing a rapid serial visual presentation (RSVP) task. The thermal stimuli were either warm or hot (individually titrated) and the task speed was adjusted for each subject to be either easy or hard (d' 70%, 16 blocks giving 4 repeats of each condition). This 2x2 factorial design allowed the interaction between task and temperature to be tested to identify the attentional analgesic effect. Each subject repeated the experiment on 3 separate days (at least one week apart) with a different drug on each occasion (naltrexone, reboxetine or placebo) and had whole CNS fMRI.

Figure 1 Supplementary Figure 1 Representative temporal signal to noise ratio (tSNR) data for a single subject, acquired with identical parameters to those used in this study. Signal optimisation included manual selection of Z-shims, based on maximisation of cord signal and minimisation of distortion at each level in the cord (Finsterbusch et al., 2012). Image data (100 samples) acquired at rest were divided at the level of the odontoid process/dens, with that above (i.e. brain) motion corrected with a rigid body approach in FSL (6.0.3) and below (i.e. cord) with 2D correction in the Spinal Cord Toolbox (5.3.0), and the outputs generated with nearest neighbour interpolation to minimise smoothing. Following motion correction, the temporal mean was calculated and divided by the temporal standard deviation to produce the tSNR map.

Figure 2 Main effect of temperature and task*temperature interaction in the spinal cord. (A) Pain scores across the four experimental conditions (i.e. easy|low, hard|low, easy|high and hard|high), for the three drugs. All conditions showed a main effect of temperature (Two-way repeated measures ANOVA). Attentional analgesia was seen in the placebo and reboxetine limbs with a task*temperature interaction ($F(1, 38) = 11.20$, $P = 0.0019$ and $F(1, 38) = 9.023$, $P = 0.004$ respectively). In both cases this was driven by lower pain scores in the hard|high versus easy|high condition (Sidak's post hoc test). In contrast Naltrexone blocked the analgesic effect of attention as reflected in a loss of the task*temperature interaction ($F(1, 38) = 0.4355$, $P = 0.5133$).

(B) Cervical spine fMRI revealed two distinct clusters of activity within the left side of the C6 cord segment. The first showing the main effect of temperature (red-yellow, $Spinal_{noci}$) and a second showing task*temperature interaction (blue-light blue, $Spinal_{int}$) (significance reported with $P<0.05$ (TFCE) within a left sided C5/C6 anatomical mask). No cluster reached significance for the main effect of task.

(C) Parameter estimates from the $Spinal_{noci}$ cluster showed a positive correlation with the pain scores across all conditions (Pearson's Correlation, 95% CI).

(D) Parameter estimates from the $Spinal_{noci}$ cluster revealed a decrease in BOLD in the hard|high versus easy|high condition, seen in placebo and reboxetine arms but not in naltrexone. Note the similarity in pattern with the pain scores in (A).

(E) Extraction of parameter estimates from the $Spinal_{int}$ cluster revealed an increase in BOLD in the hard|high condition, across all three drug sessions compared to the easy|high and hard|low conditions (Friedman test $P<0.0001$).

Mean±SEM. Parameter estimates extracted from the peak voxel in each cluster.

Figure 2 Supplementary Figure 1 Pain scores under the four experimental conditions (i.e. easy|low, hard|low, easy|high and hard|high), across the three drugs for each of the 39 subjects. A first level, three-way repeated measures ANOVA revealed the expected main effect of temperature (F (1,38) = 221, P=0.0001), main effect of task (F (1,38) = 4.9, P=0.03) and importantly a task*temperature interaction (F (1, 38) = 10.5, P = 0.0025). The first level analysis also showed a drug*temperature interaction on pain ratings (F (2, 76) = 3.2, P = 0.04). To further investigate the drug*temperature interaction, two second level three-way repeated measures ANOVAs were conducted for placebo vs reboxetine and placebo vs naltrexone (Figure 2). For reboxetine versus placebo, a drug*temperature interaction was revealed (F (1, 38) = 5.060, P = 0.03), with lower pain scores in high temperature condition in the reboxetine arm, indicating an analgesic effect of the drug. No drug*temperature interactions were observed in the ANOVA contrasting naltrexone with placebo. Mean+SEM with individual participants data.

Figure 2 Supplementary Figure 2

A) Attentional analgesia effect reflected as the difference in pain score between the easy and hard condition in the high temperature condition (mean ± 95% confidence interval). The placebo and reboxetine groups show a significant reduction in pain scores in the high hard condition ie attentional analgesia (P=0.0016 and P=0.013 respectively) whereas there is no significant effect of naltrexone (P=0.51, one sample t-tests). The corresponding effect sizes (Cohen's Dz) are Placebo -0.55, Reboxetine -0.42 vs Naltrexone -0.11. The confidence interval for naltrexone spans zero and equivalence testing showed that the magnitude of the effect was smaller than a 6% (2.3 point) reduction in pain score (P=0.049, using the TOST approach (Lakens, 2017)) and less than the analgesic effect seen in the presence of reboxetine or placebo.

B) Extraction of the BOLD parameter estimates from the $Spinal_{noci}$ cluster for the HH-EH conditions showed a similar pattern of means but with an increased dispersion of values (note the break in the y-axis scale) reflecting the signal to noise associated with spinal cord functional imaging. As a consequence, the 95% confidence intervals all cross zero and there are no significant differences between the groups.

C) Extraction of the BOLD parameter estimates from the $Spinal_{int}$ cluster for the High Hard condition showed that the group means were significantly increased in the placebo (P=0.018) and reboxetine (P=0.0018) conditions but not in the presence of naltrexone (P=0.24). (Mean±95% CI, one sample t-tests).

Figure 2 Supplementary Figure 3 Temperature delivered and task speed across the three drug conditions. (A) Administration of Reboxetine or Naltrexone did not change the individually calibrated HIGH thermal stimulus required to evoke a 6/10 pain score (Mean ± SD). (B) Similarly, drug administration had no effect on RSVP task speed as reflected in the inter-character presentation interval. (Mean ±SD, Friedman tests NS).

Figure 2 Supplementary Figure 4 Analysis of pooled data for main effects and interaction within the cord. Top: PAM50 template T1-weighted cervical cord, bottom: mean functional image from all 39 subjects acquired during the placebo condition, shown following non-linear registration to the template. Note the good agreement with intervertebral disc levels and ventral surface of the cord. The registration pipeline included two steps: (1) registration of subject's own T1-weighted structural scan to PAM50 T1-weighted template, (2) registration of acquired functional images to PAM50 template (T2*-weighted) to using the output from step 1 as an initial warping. This last step assumed that the subject's T1-

weighted scan and EPI data were in reasonable agreement, which was confirmed by visual inspection. Note that in every case it was found that manual intervention was required to improve the cord mask for the functional images.

Figure 2 Supplementary Figure 5 Analysis of pooled data for main effects and interaction within the cord. Inference was performed without masking for a specific vertebral level and produced t-scores shown in Red-Yellow (positive) and Blue-Light blue (negative). Importantly, the unmasked analysis confirmed the presence of a main effect of temperature at the C5/C6 level within the left dorsal horn region (shown in Green, with cross-hair on voxel of with lowest p-value), with TFCE corrected $P<0.05$. Similarly, unmasked analysis provided confirmatory evidence for the existence of a task x temperature interaction located within the left dorsal horn region at the C5/C6 level (Green, cross-hair on voxel with lowest p-value), with TFCE corrected $P<0.05$. No main effect of task was observed within the cord, in agreement with masked analysis.

Figure 2 Animation 1 Registration of functional imaging data to PAM50 template cord. Overlaid PAM50 template T1-weighted cervical cord and mean functional image from all 39 subjects acquired during the placebo condition, shown following non-linear registration to the template. Note the good agreement with intervertebral disc levels and ventral surface of the cord. Note the cross hair marks the midline of the ventral surface of the spinal cord in both anatomical and functional images.

Figure 3 Main effect of task and temperature in Brainstem and Cerebrum.

(A) Main effect of temperature and task in the brainstem after permutation testing with a whole brainstem mask showing clusters of activation in PAG, bilateral LC and RVM. Activity reported with corrected $P<0.05$ (TFCE).

(B) Main effects of temperature and task in brain. In the main effect of temperature contrast there were clusters of activation in a number of pain related sites including in the contralateral primary somatosensory cortex, the dorsal posterior insula and the PAG (red-yellow). The frontal medial cortex de-activated (blue-light blue). In the main effect of task contrast there were clusters of activation in the visual and attention networks including superior parietal cortex, the frontal pole, and the anterior cingulate cortex (red-yellow). The posterior cingulate cortex and lateral occipital cortex showed de-activation (blue-light blue). Activity was estimated with a cluster forming threshold of $Z>3.1$ and FWE corrected $P<0.05$.

(PAG – Periaqueductal grey, LC – Locus coeruleus, RVM – Rostral ventromedial medulla, FMC – Frontomedial cortex, dpIns – dorsal posterior insula, SI – primary somatosensory cortex, LOC – Lateral ocipital cortex (sup and inf), SPL Superior parietal lobule.)

Figure 3 Supplementary Figure 1 Whole brain mixed effects analysis of pooled data (inputs are the average of each subject's 3 sessions) for the 3 contrasts (main effects of temperature, task and their interaction). Slices shown (left to right) (i) midline sagittal, (ii) coronal through the PAG, bilateral LC and RVM masks, and (iii) axial at the level of the midline RVM mask. To allow visualisation of underlying anatomy, data were thresholded at an uncorrected P-value of 0.05 (i.e. $Z>1.65$). The location of relevant masks are outlined in white, with labels shown. Also included is the brainstem mask derived from the Harvard-Oxford sub-cortical probabilistic atlas, which was thresholded at 50% and used for estimating brainstem activity reported in the manuscript (rather than the whole brain analysis shown here). Assignment of activity to specific nuclei was based on overlap with

probabilistic brainstem nuclei masks (Brooks et al., 2017). Positive Z-scores are shown in Red-Yellow colours, whilst negative ones are in Blue-Light blue. Activity was rarely observed in the 4th ventricle, nor in the aqueduct, indicating that physiological noise was adequately corrected for with the chosen scheme (see (Brooks et al., 2008; Kong et al., 2012) for more details).

Figure 3 Supplementary Figure 2 Anterior Insula and medulla response after Naltrexone administration. (A) The anterior insula responded more strongly in the naltrexone than in the placebo in the main effect of task (obtained with permutation testing with a main effect of task mask, obtained from the pooled analysis). (B) A cluster in the lower medulla responded more strongly in the naltrexone than in the placebo main effect of temperature. Result obtained with permutation testing (using a main effect of temperature brainstem mask, obtained from the pooled analysis). TFCE corrected $P<0.05$.

Figure 4 Summary of significant connection changes revealed by the gPPI analysis (placebo condition only). (A) Permutation testing revealed a significant change in connectivity in the main effect of task contrast between ACC and PAG, and in the task*temperature interaction contrast between PAG and RVM, LC and RVM, and importantly RVM and spinal cord. Masks used for time-series extraction are shown in the sagittal slice (yellow). The spinal cord axial slice shows the voxels with significantly connections with RVM (threshold at $P = 0.1$ for visualization purposes). (B) Extraction of parameter estimates revealed an increase in coupling in the analgesic condition for all of these connections (i.e. hard|high). (Mean ± SEM).

Figure 4 Supplementary Figure 1 Unmasked whole brain group data for effective connectivity analysis of the placebo condition only. For each subject the seed was extracted for the main effect of temperature (within the pooled simple main effects data) within the RVM. I.e. a functional mask was derived from the group data, masked anatomically then applied to each subject separately to identify their peak voxel time series (the seed). Subsequently, the connectivity profile was estimated for each subject using generalised psychophysiological analysis (gPPI), with separate contrasts between the gPPI regressors for the 3 conditions (main effects of task, temperature and their interaction). To allow visualisation of underlying anatomy, these whole brain data were thresholded at an uncorrected P-value of 0.05 (i.e. $Z>1.65$). The location of relevant masks are outlined in white (see labels on previous brainstem figure). Positive Z-scores are shown in Red-Yellow colours, whilst negative ones are in Blue-Light blue.

Figure 4 Supplementary Figure 2 Unmasked group cord data from connectivity analysis of the placebo condition shown on the PAM50 spinal cord template. For each subject the physiological regressor was extracted from a functional mask representing the main effect of temperature within the RVM for the placebo condition. Subsequently, generalised psychophysiological interaction (gPPI) regressors were formed for each of the conditions and contrasts between them created. The data represent uncorrected positive (Red-Yellow) and negative (Blue-Lightblue) t-scores, which are the output from RANDOMISE. Vertebral levels are indicated on sagittal section (left side of image). Due to masking steps in the registration pipeline it was not possible to include tissues outside the cord. To aid interpretation of the patterns of activity, the left C5-C6 vertebral mask is shown (white

outline). Significant group activity detected within the mask for each contrast are shown in green, with TFCE corrected P<0.05.

Figure 5 Alteration of functional connectivity after dosing with naltrexone or reboxetine compared to placebo. The ACC-PAG connection was significantly weakened by Naltrexone and Reboxetine administration. The RVM-spinal cord connection was significantly weakened by Naltrexone. Red crosses indicate significantly weaker connections after drug. Inset bar plots show BOLD parameter estimates extracted from the PAG-ACC and RVM-spinal cord connections. (Means±SEM, paired t-test, *P<0.05).

Figure 1

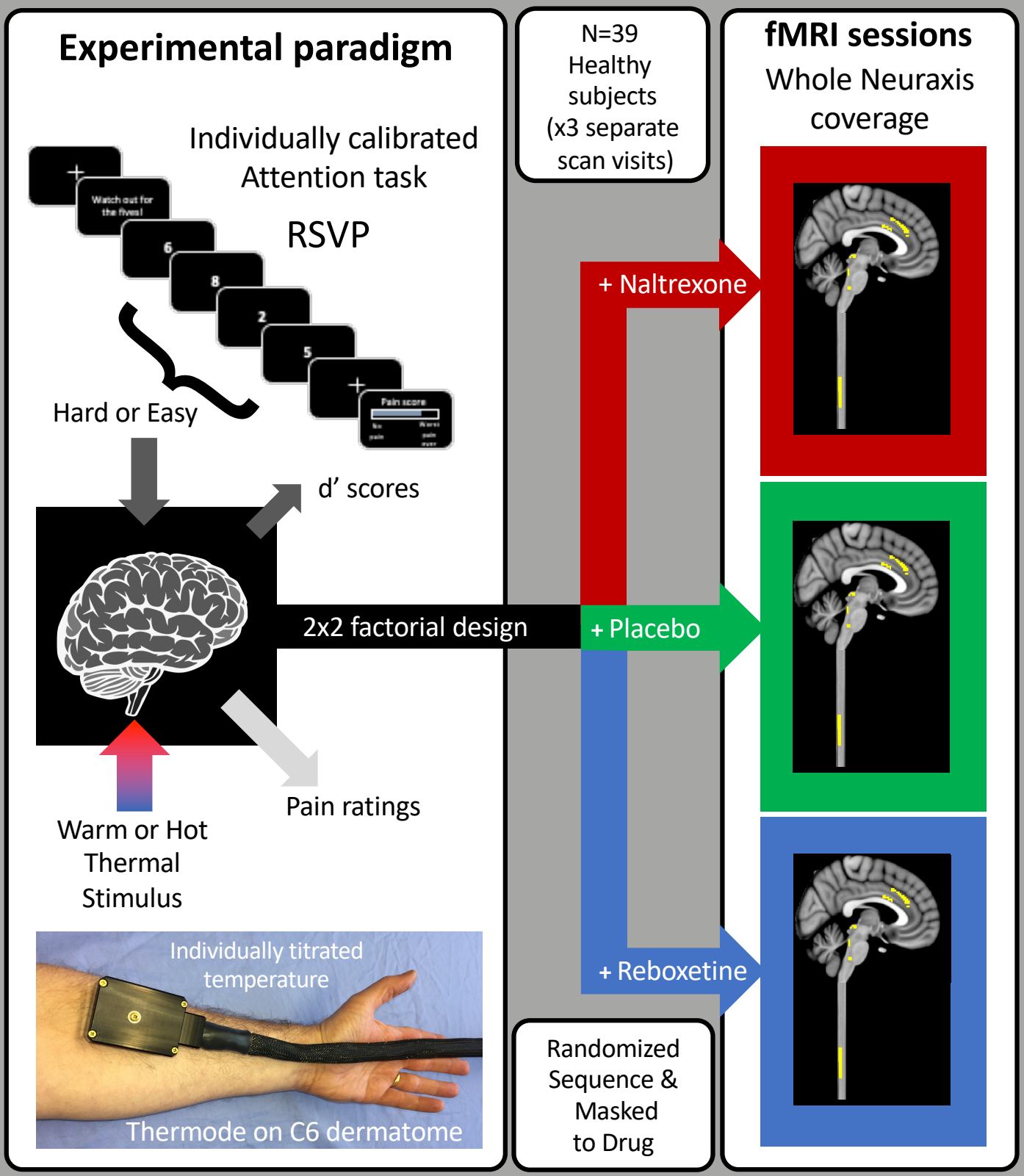
Experimental paradigm
Individually calibrated Attention task
RSVP
Watch out for the fives!
Pain score
Hard or Easy
d' scores
2x2 factorial design
Pain ratings
Warm or Hot Thermal Stimulus
Individually titrated temperature
Thermode on C6 dermatome
N=39 Healthy subjects (x3 separate scan visits)
+ Naltrexone
+ Placebo
+ Reboxetine
Randomized Sequence & Masked to Drug
fMRI sessions
Whole Neuraxis coverage

Figure 1 Supplementary Figure 1

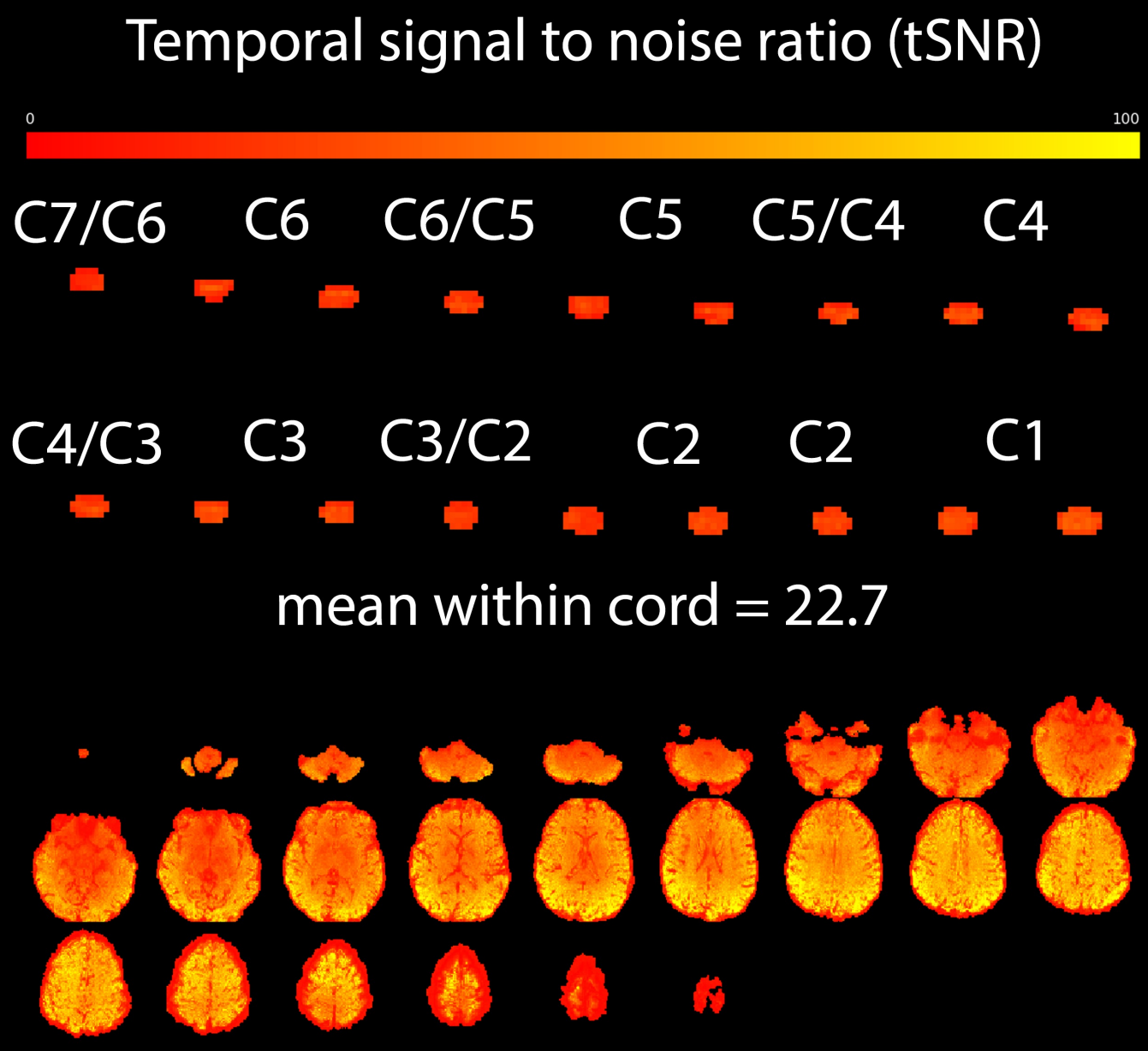

Figure 2

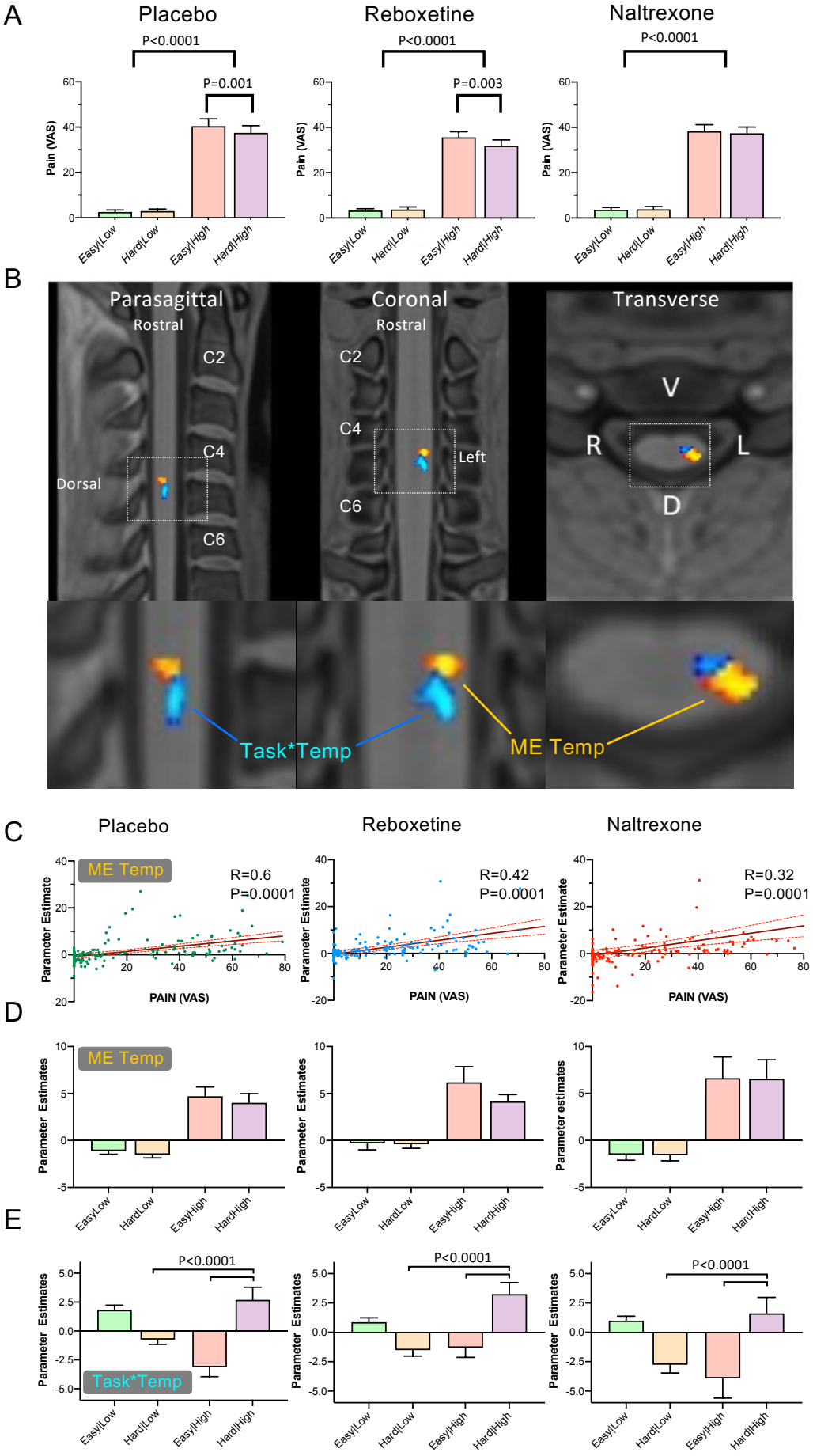
A
Placebo
Reboxetine
Naltrexone
P<0.0001
P=0.001
P=0.003
Pain (VAS)
EasyLow
HardLow
EasyHigh
HardHigh
B
Parasagittal
Rostral
C2
C4
C6
Dorsal
Coronal
Left
Transverse
V
R
L
D
Task*Temp
ME Temp
C
Placebo
Reboxetine
Naltrexone
ME Temp
R=0.6
P=0.0001
R=0.42
P=0.0001
R=0.32
P=0.0001
Parameter Estimate
PAIN (VAS)
D
ME Temp
Parameter Estimates
Parameter estimates
E
P<0.0001
Task*Temp
Parameter Estimates

Figure 2 Supplementary Figure 1

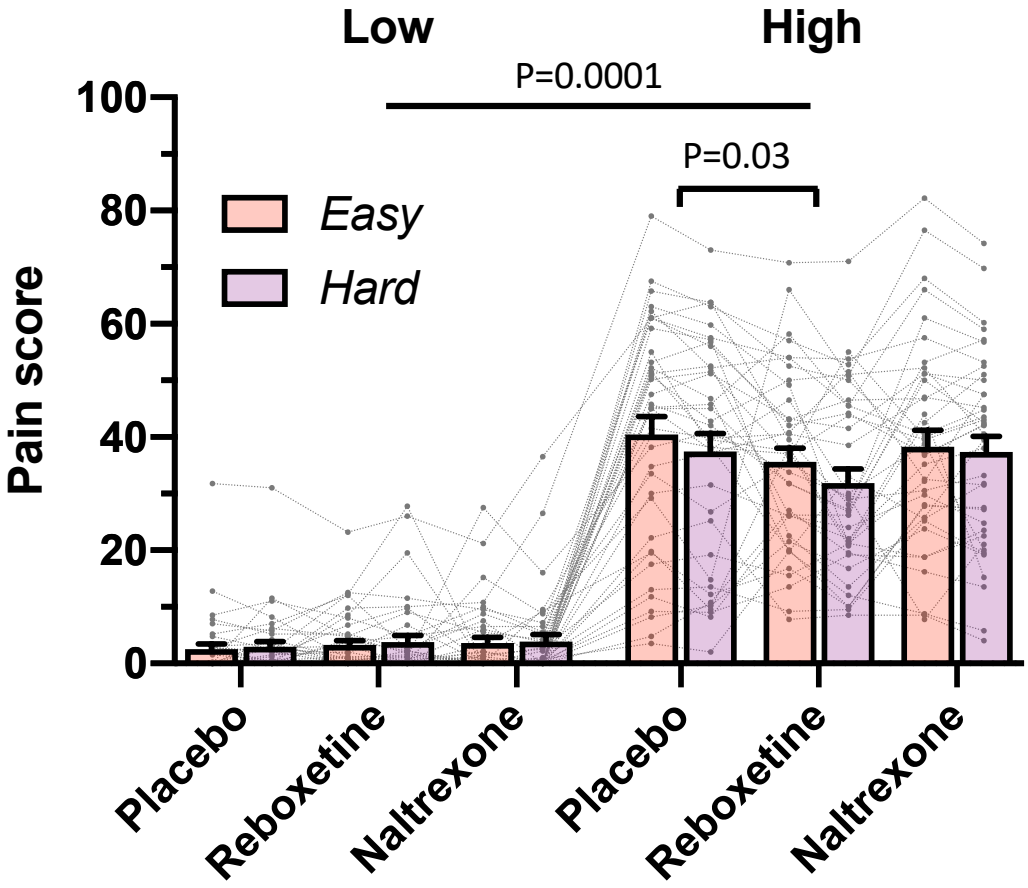

ANOVA table	F (DFn, DFd)	P value
Drug	F (2, 76) = 2.272	P=0.11
Temperature	F (1, 38) = 221.6	P<0.0001
Task	F (1, 38) = 4.869	P=0.034
Drug x Temperature	F (2, 76) = 3.243	P=0.045
Drug x Task	F (2, 76) = 1.210	P=0.30
Temperature x Task	F (1, 38) = 10.50	P=0.0025
Drug x Temperature x Task	F (2, 76) = 1.579	P=0.21

Figure 2 Supplementary Figure 2

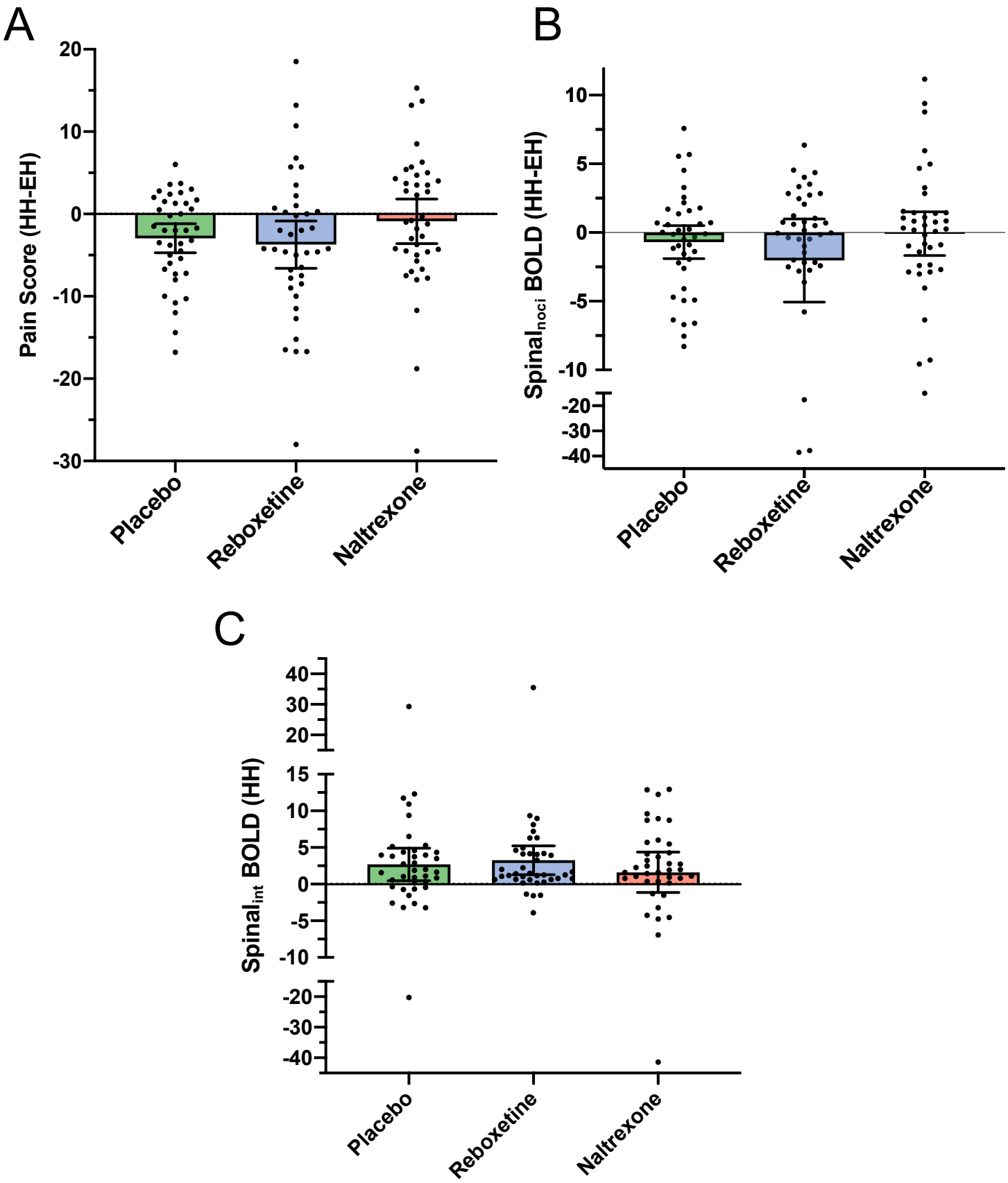

Figure 2 Supplementary Figure 3

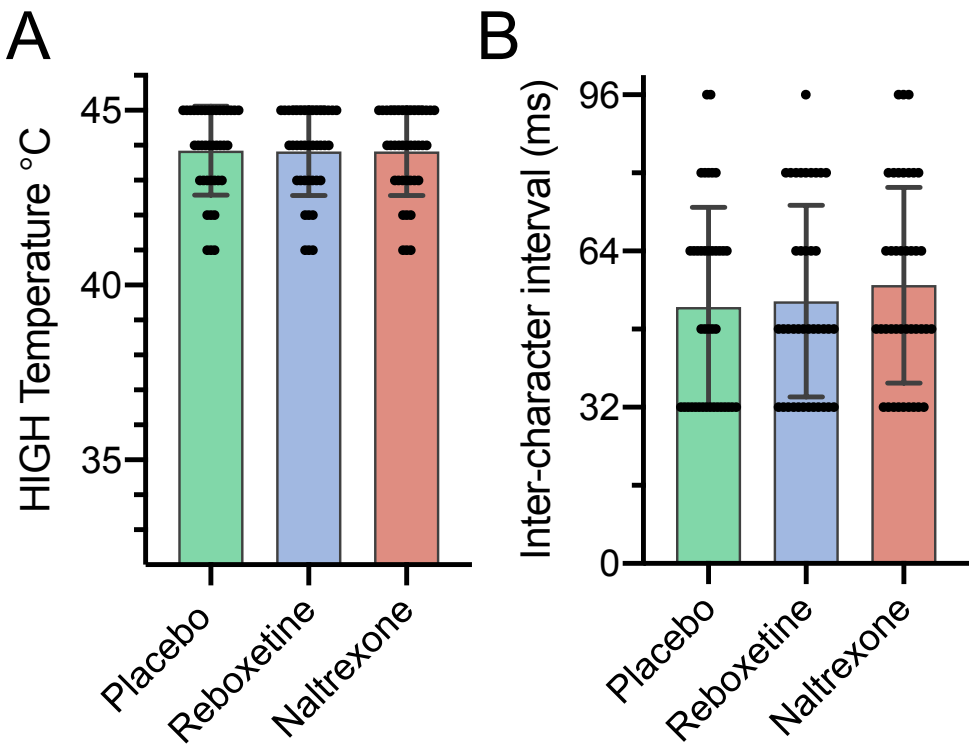

Figure 2 Supplementary Figure 4

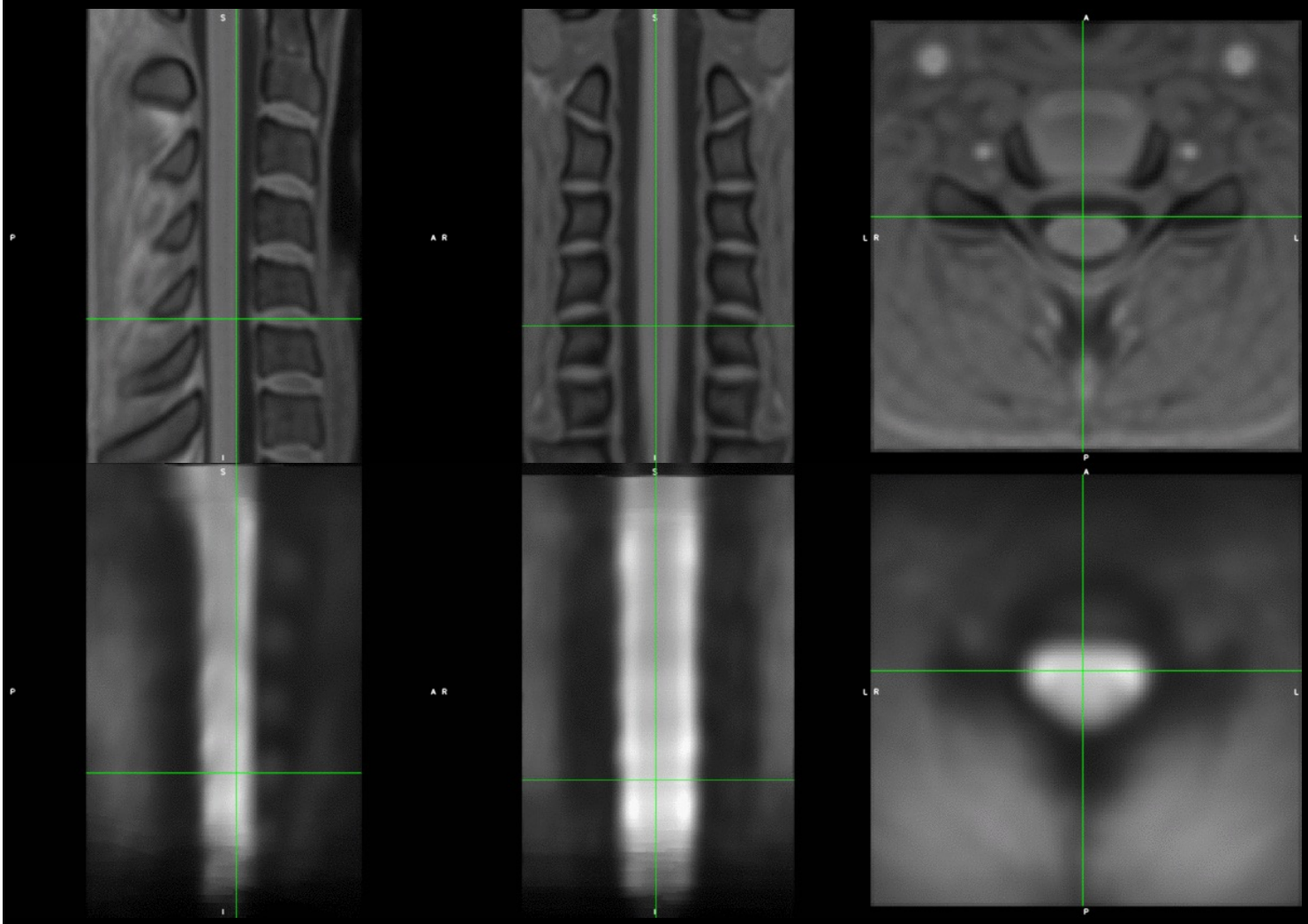

Figure 2 Supplementary Figure 5

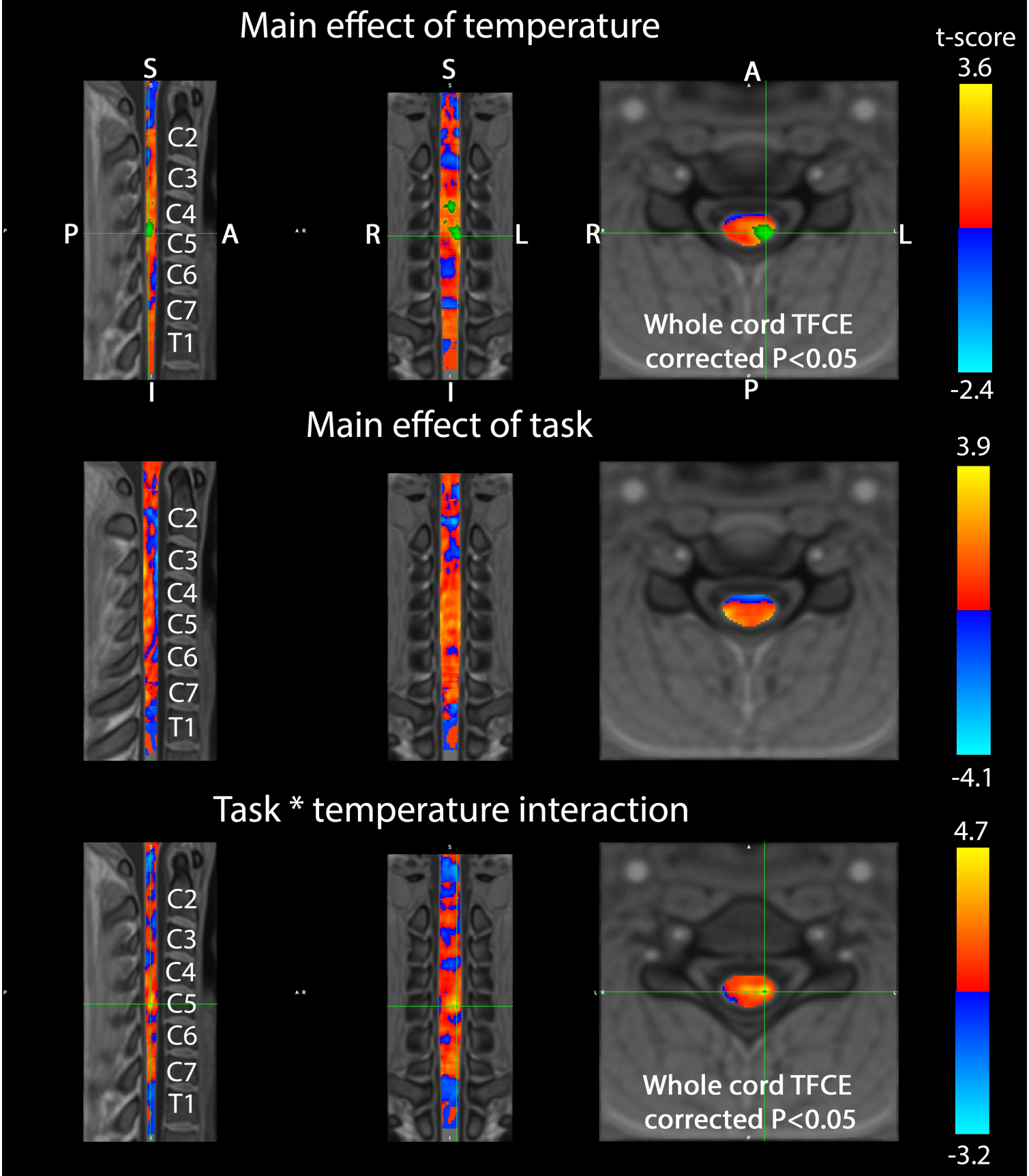

Figure 3

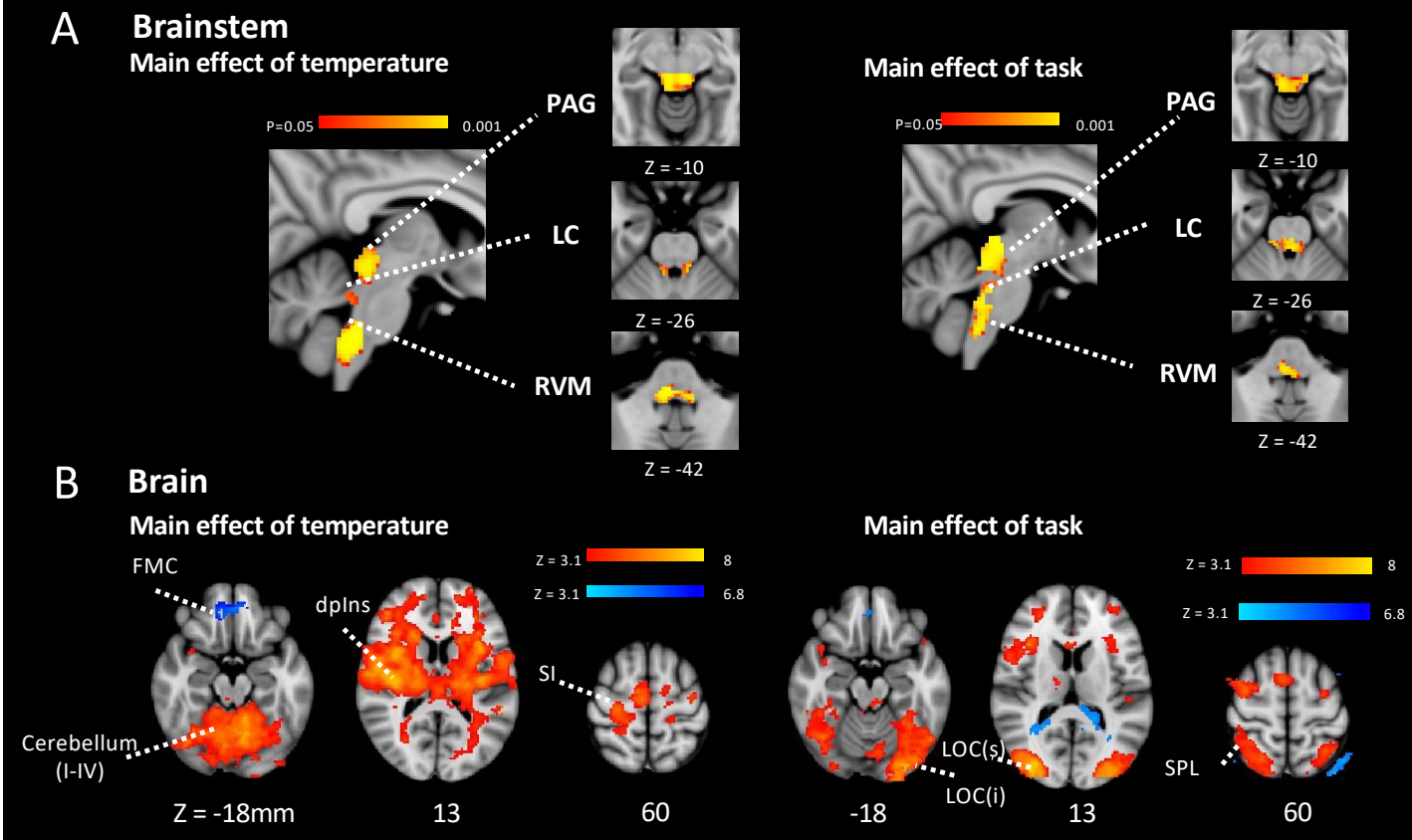
A
Brainstem
Main effect of temperature
P=0.05
0.001
PAG
LC
RVM
Z = -10
Z = -26
Z = -42
Main effect of task
P=0.05
0.001
PAG
LC
RVM
Z = -10
Z = -26
Z = -42
B
Brain
Main effect of temperature
FMC
dpIns
SI
Cerebellum
(I-IV)
Z = 3.1
8
Z = 3.1
6.8
Z = -18mm
13
60
Main effect of task
LOC(s)
LOC(i)
SPL
Z = 3.1
8
Z = 3.1
6.8
-18
13
60

Figure 3 Supplementary Figure 1

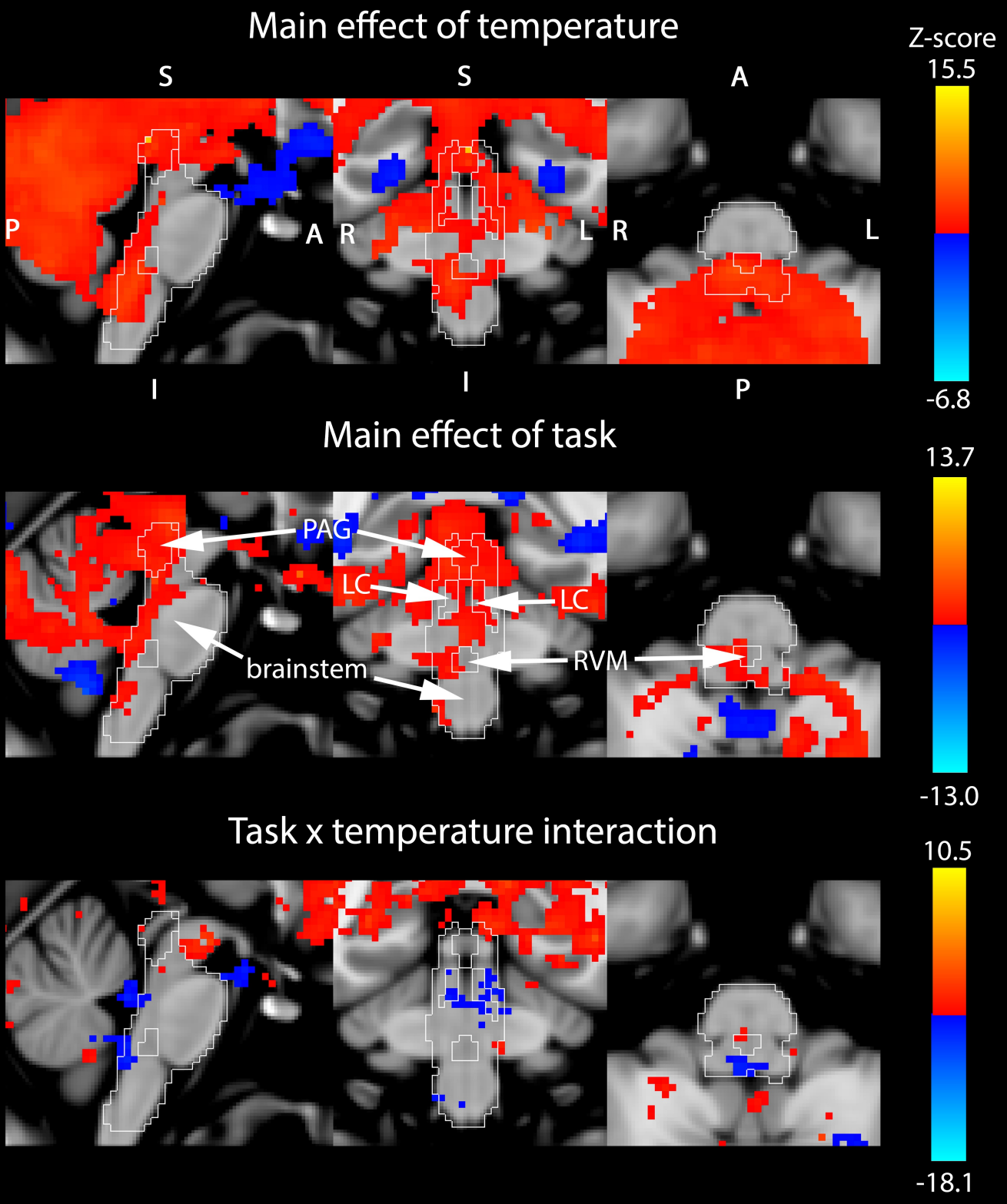

Figure 3 Supplementary Figure 2

A

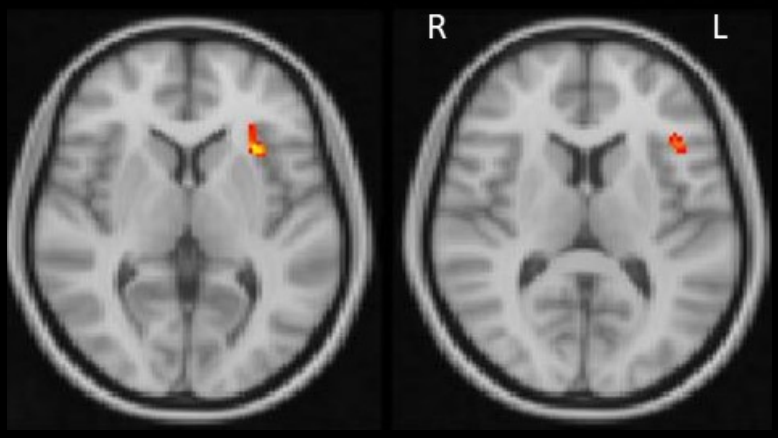

B

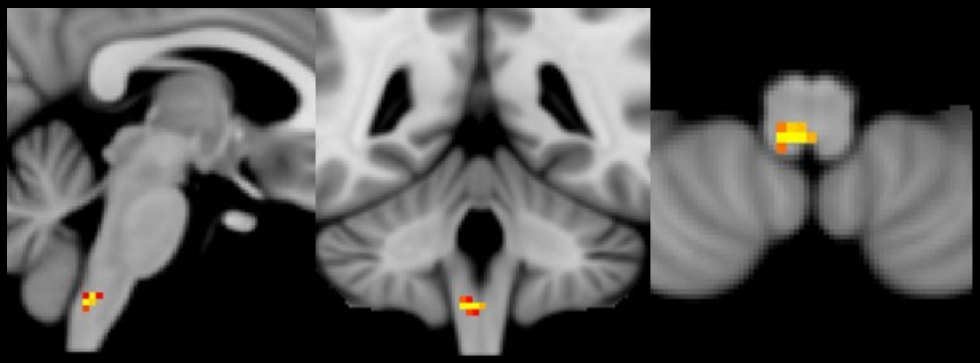

Figure 4

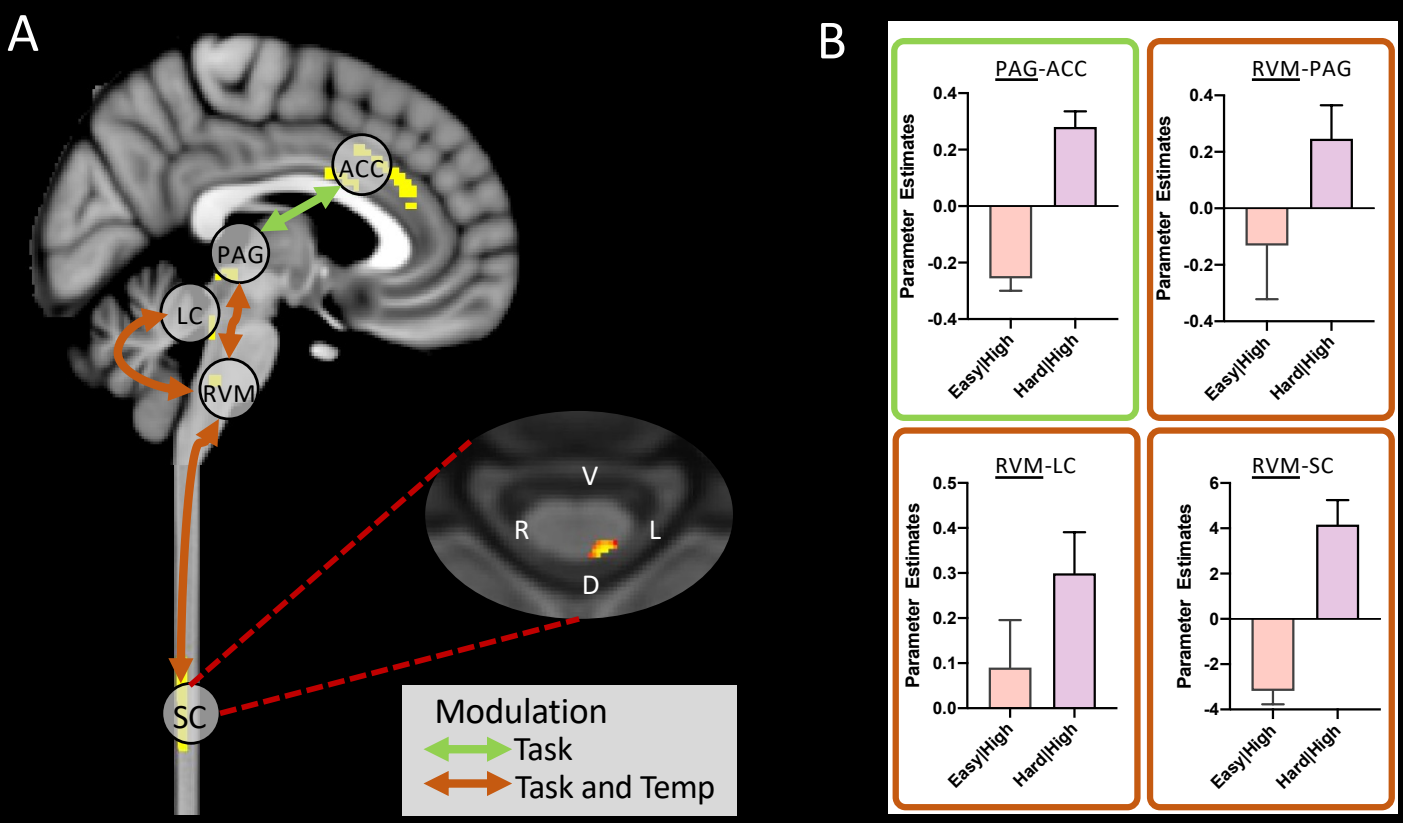
A
ACC
PAG
LC
RVM
SC
V
R
L
D
Modulation
Task
Task and Temp
B
PAG-ACC
RVM-PAG
RVM-LC
RVM-SC
Parameter Estimates
Easy|High
Hard|High

Figure 4 Supplementary Figure 1

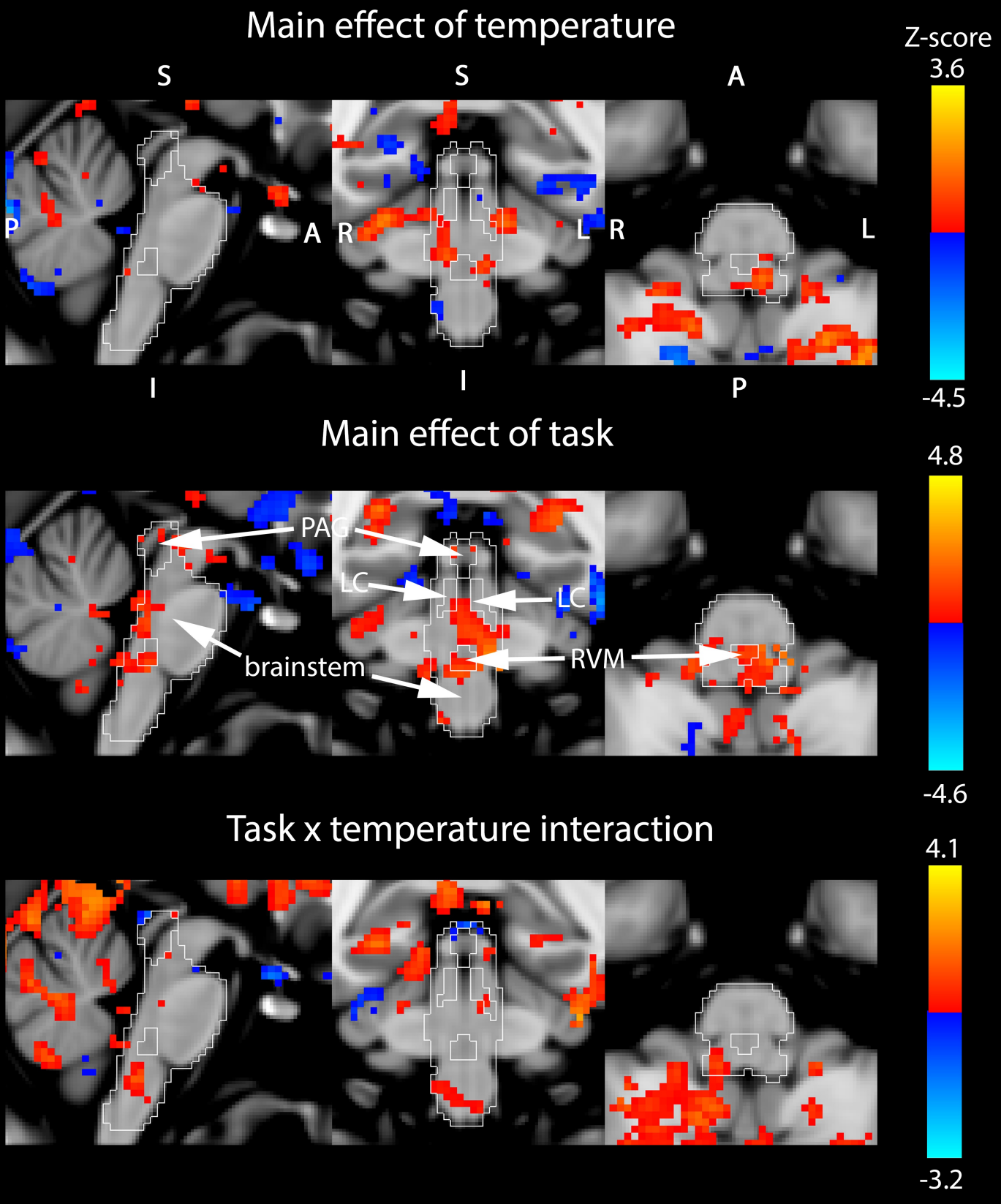

Figure 4 Supplementary Figure 2

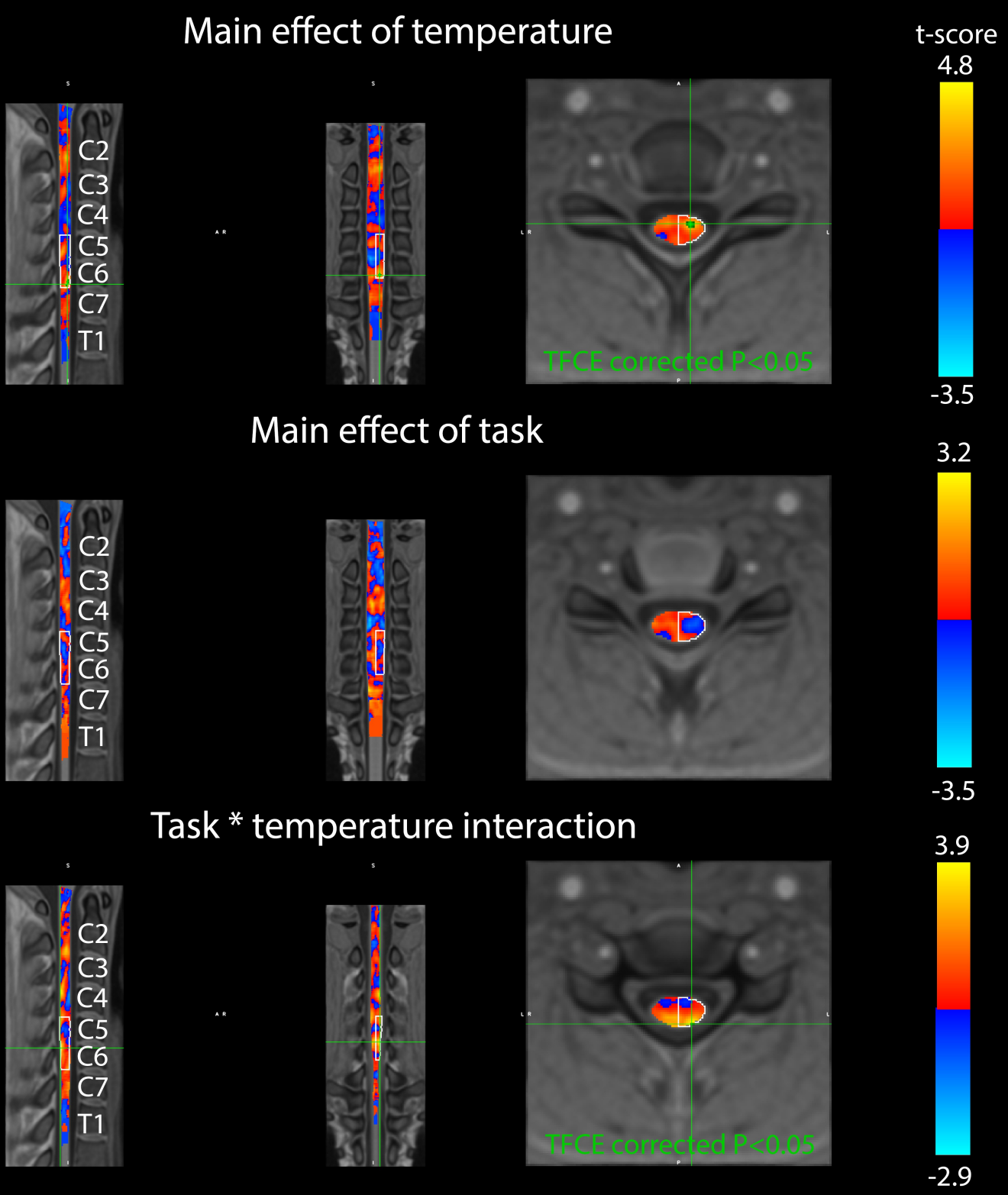

Figure 5

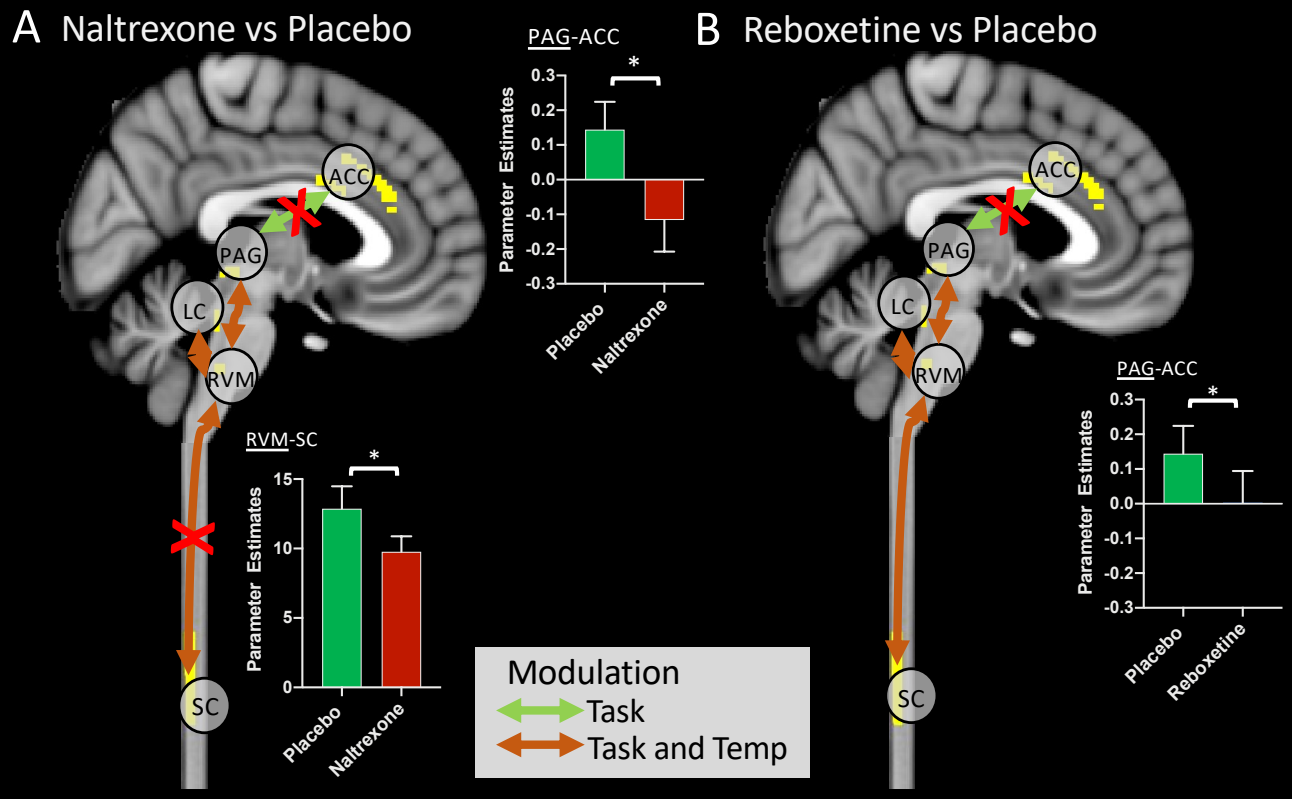
A Naltrexone vs Placebo
ACC
PAG
LC
RVM
SC
PAG-ACC
Parameter Estimates
0.3
0.2
0.1
0.0
-0.1
-0.2
-0.3
*
Placebo
Naltrexone
RVM-SC
15
10
5
0
Modulation
Task
Task and Temp
B Reboxetine vs Placebo
Reboxetine